Nanoparticles and biochar with adsorbed plant growth-promoting rhizobacteria alleviate Fusarium wilt damage on tomato and watermelon

Milica Pavlicevic, Wade Elmer, Nubia Zuverza-Mena, Wael Abdelraheem, Ravikumar Patel, Christian Dimpka, Tana O'Keefe, Christy L. Haynes, Luca Pagano, Marina Caldara, Marta Marmioli, Elena Maestri, Nelson Marmiroli, Jason C. White

PII: S0981-9428(23)00563-6

DOI: https://doi.org/10.1016/j.plaphy.2023.108052

Reference: PLAPHY 108052

To appear in: Plant Physiology and Biochemistry

Received Date: 10 June 2023

Revised Date: 17 September 2023 Accepted Date: 20 September 2023

Please cite this article as: M. Pavlicevic, W. Elmer, N. Zuverza-Mena, W. Abdelraheem, R. Patel, C. Dimpka, T. O'Keefe, C.L. Haynes, L. Pagano, M. Caldara, M. Marmioli, E. Maestri, N. Marmiroli, J.C. White, Nanoparticles and biochar with adsorbed plant growth-promoting rhizobacteria alleviate Fusarium wilt damage on tomato and watermelon, *Plant Physiology et Biochemistry* (2023), doi: https://doi.org/10.1016/j.plaphy.2023.108052.

This is a PDF file of an article that has undergone enhancements after acceptance, such as the addition of a cover page and metadata, and formatting for readability, but it is not yet the definitive version of record. This version will undergo additional copyediting, typesetting and review before it is published in its final form, but we are providing this version to give early visibility of the article. Please note that, during the production process, errors may be discovered which could affect the content, and all legal disclaimers that apply to the journal pertain.

© 2023 Published by Elsevier Masson SAS.



Author Contribution Statement

Milica Pavlicevic: Conceptualization; Formal analysis; Investigation; Validation; Writing-original Draft; Visualization.

Wade Elmer: Conceptualization; Formal analysis; Investigation; Resources; Data Curation; Writing-Review & Editing.

Nubia Zuverza-Mena: Formal analysis; Investigation; Data Curation; Writing- Review & Editing.

Wael Abdelraheem: Formal analysis; Investigation; Data Curation; Writing- Review & Editing. **Ravikumar Patel:** Formal analysis; Investigation; Writing- Review & Editing.

Christian Dimpka: Conceptualization; Validation; Resources; Data Curation; Writing- Review & Editing.

Tana O'Keefe: Data Curation; Resources; Visualization; Writing- Review & Editing.

Christy L. Haynes: Data Curation; Resources; Visualization; Writing- Review & Editing.

Luca Pagano: Data Curation; Visualization; Writing- Review & Editing.

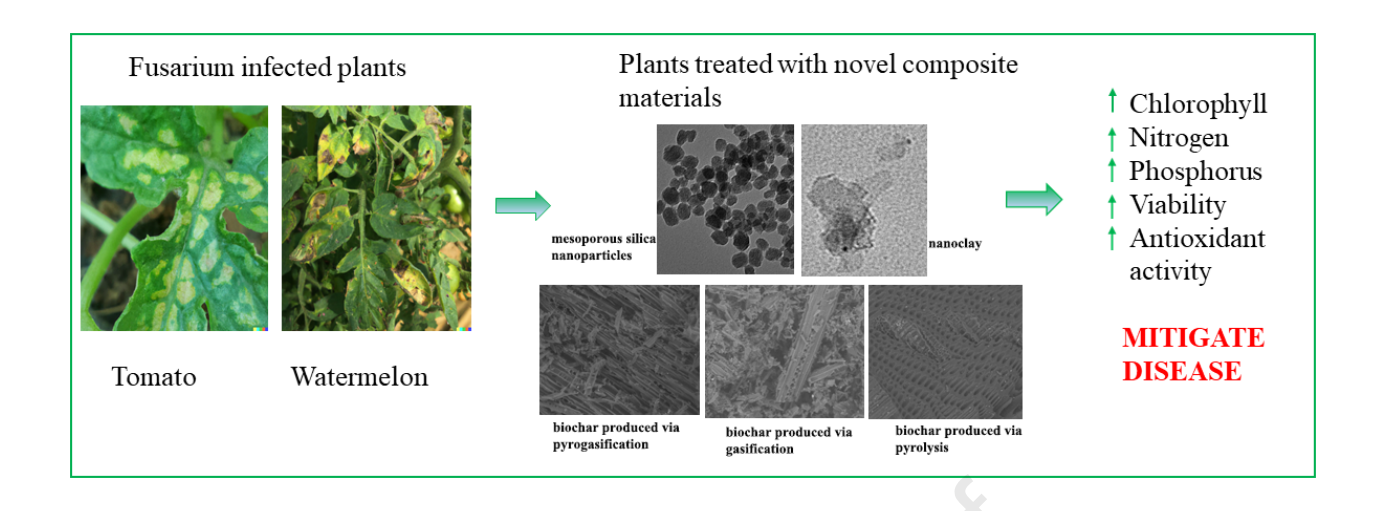
Marina Caldara: Data Curation; Visualization; Writing- Review & Editing.

Marta Marmioli: Data Curation; Visualization; Writing- Review & Editing.

Elena Maestri: Conceptualization; Data Curation; Supervision; Funding acquisition; Project administration; Writing-Review & Editing.

Nelson Marmiroli: Conceptualization; Data Curation; Supervision; Funding acquisition; Writing-Review & Editing.

Jason C. White: Conceptualization; Resources; Data Curation; Supervision; Funding acquisition; Project administration; Writing- Review & Editing.



1 Nanoparticles and biochar with adsorbed plant growth-promoting rhizobacteria alleviate

- 2 Fusarium wilt damage on tomato and watermelon
- 3 Milica Pavlicevic^{1*}, Wade Elmer², Nubia Zuverza-Mena², Wael Abdelraheem^{2,3}, Ravikumar
- 4 Patel², Christian Dimpka², Tana O'Keefe⁴, Christy L. Haynes⁴, Luca Pagano¹, Marina Caldara¹,
- 5 Marta Marmioli¹, Elena Maestri^{1,5}, Nelson Marmiroli^{1,5,6} and Jason C. White²
- 6 Department of Chemistry, Life Sciences and Environmental Sustainability, University of Parma,
- 7 Parma, Italy; <u>milica.pavlicevic@unipr.it</u> (M.P.); <u>luca.pagano@unipr.it</u> (L.P.);
- 8 <u>marina.caldara@unpr.it</u> (M.C.); <u>marta.marmiroli@unipr.it</u> (M.M); <u>elena.maestri@unipr.it</u> (E.M.);
- 9 <u>nelson.marmiroli@unipr.it</u> (N.M.)
- ² Connecticut Agricultural Experimental Station, New Haven, CT, USA; <u>Nubia.Zuverza@ct.gov</u>
- 11 (N.Z.M.); whafez2008@gmail.com (W.A.); Wade.Elmer@ct.gov (W.E.);
- 12 <u>Ravikumar.Patel@ct.gov</u> (R.P.), <u>Christian.Dimkpa@ct.gov</u> (C.D.), <u>Jason.White@ct.gov</u> (J.C.W.)
- ³ Chemistry Department, Faculty of Science, Sohag University, Sohag 82524, Egypt;
- whafez2008@gmail.com

- Department of Chemistry, University of Minnesota, Minneapolis, MN, USA;
- 17 <u>okeef179@umn.edu</u> (T.O.); <u>chaynes@umn.edu</u> (C.H.)
- ⁵ Interdepartmental Center SITEIA.PARMA, University of Parma, Parma, Italy;
- 19 <u>elena.maestri@unipr.it</u> (E.M.); <u>nelson.marmiroli@unipr.it</u> (N.M.)
- 20 6 National Interuniversity Consortium for Environmental Sciences (CINSA), Parma, Italy;
- 21 <u>nelson.marmiroli@unipr.it</u>
- * Correspondence: milica.pavlicevic@unipr.it; Tel: +393474067069

Abstract: The addition of biochars and nanoparticles with adsorbed *Azotobacter vinelandii* and Bacillus megaterium alleviated damage from Fusarium infection in both tomato (Solanum lycopersicum) and watermelon (Citrullus lanatus) plants. Tomato and watermelon plants were grown in greenhouse for 28 and 30 days (respectively) and were treated with either nanoparticles (chitosan-coated mesoporous silica or nanoclay) or varying biochars (biochar produced by pyrolysis, gasification and pyrogasification). Treatments with nanoparticles and biochars were applied in two variants - with or without adsorbed plant-growth promoting bacteria (PGPR). Chitosan-coated mesoporous silica nanoparticles with adsorbed bacteria increased chlorophyll content in infected tomato and watermelon plants (1.12 times and 1.63 times, respectively) to a greater extent than nanoclay with adsorbed bacteria (1.10 times and 1.38 times, respectively). However, the impact on other endpoints (viability of plant cells, phosphorus and nitrogen content, as well antioxidative status) was species-specific. In all cases, plants treated with adsorbed bacteria responded better than plants without bacteria. For example, the content of antioxidative compounds in diseased watermelon plants increased nearly 46% upon addition of Aries biochar and by approximately 52% upon addition of Aries biochar with adsorbed bacteria. The overall effect on disease suppression was due to combination of the antifungal effects of both nanoparticles (and biochars) and plant-growth promoting bacteria. These findings suggest that nanoparticles or biochars with adsorbed PGPR could be viewed as a novel and sustainable solution for management of Fusarium wilt.

Keywords: nanoclay; mesoporous silica; biochar; PGPR; Fusarium

43

44

23

24

25

26

27

28

29

30

31

32

33

34

35

36

37

38

39

40

41

42

1. Introduction

- The economic and environmental impact of plant diseases caused by different formae speciales of
- 46 Fusarium oxysporum is significant (Okungbowa and Shittu, 2012; Epstein et al., 2022; Figueiredo

Silva et al., 2023). Globally, each year Fusarium wilt decreases production of rice (*Oryza sativa*) 47 by 25% - 41%, wheat (Triticum durum) by 10% - 28%, and soybean (Glycine max) by 11% -48 32%, etc. (Figueiredo Silva et al., 2023). Due to sensitivity of bananas (Musa sp.) to Fusarium 49 oxysporum f.sp. cubense Tropical race 4, 111 billion US dollars were "lost" in 2016 (Figueiredo 50 Silva et al., 2023). Crop species subject to Fusarium attack include most major food crops, such 51 52 as wheat, soybean, yam (Dioscorea sp.), oats (Avena sativa), etc. (Adisa et al., 2018; Cai et al., 2020; Dongzhen et al., 2020; Havrlentová et al., 2021; Yang et al., 2022). Although fungicides can 53 effectively manage select fungal plant pathogens (Mondani et al., 2021), efficacy against Fusarium 54 55 diseases is highly limited (due to their relatively low efficacy as demethylation inhibitors and quinone outside inhibitors), and negative impacts on the environment are significant (González-56 Domínguez et al., 2021; Lin et al., 2019; Mahmood et al., 2016). Notably, leaf extracts of medicinal 57 plants (such as Azadirachta indica, Punica granatum, and Pinus wallachiana) have shown 58 antifungal activity, both when applied in the seedling phase and when added directly to the soil 59 (Abo-Elyousr et al., 2022; Ain et al., 2022). Thus, more environment-friendly solutions to manage 60 F. oxysporum infection have been investigated, such as the application of nanoparticles, biochar, 61 and specific microorganisms as soil additives (Buchman et al., 2019; Egamberdieva et al., 2020; 62 63 Jaiswal et al., 2020; Saleh et al., 2021; Chen et al., 2023). 64 Indeed, different metallic and metallic oxide nanoparticles (such as Ag, Cu, Ni, Mn, CeO₂, CuO 65 nanoparticles), as well as nanocomposites (such as nanoscale hydroxyapatite) and silica 66 nanoparticles, have all been used successfully to suppress or delay damage from F. oxysporum infection of tomato and watermelon (Ahmed et al., 2016; Adisa et al., 2018; Buchman et al., 2019; 67 68 Kang et al., 2021; Ahmad et al., 2022; Shah et al., 2022; Noman et al., 2023). Although reduction 69 of disease strongly depends on the type of plant examined, the average disease reduction was in

70

71

72

73

74

75

76

77

78

79

80

81

82

83

84

85

86

87

88

89

90

91

92

the range of 53 -84.5% (Ahmed et al., 2016; Adisa et al., 2018; Buchman et al., 2019; Shah et al., 2022). Chitosan, often used as biocompatible nanoparticle coating material, also exhibits direct antifungal activity (Carmona et al., 2021; Wahyuni et al., 2021) and induces the activation of plant defense pathways (Katiyar et al., 2015). Carmona et al. (2021) reported that chitosan-treated plants showed higher expression of the PR1a gene that codes for a protein associated with the accumulation of the important defense biomolecule, salicylic acid. The mechanisms by which nanoparticles suppress F. oxysporum infection are unclear, but are typically dependent on nanoparticle type and properties. For example, Adisa et al. (2018) correlated the antifungal activity of CeO₂ nanoparticles with their ability to counteract the negative effect of free radical species produced by F. oxysporum f. sp. lycopersici. Ahmad et al. (2022) and Lopez-Lima et al. (2021) also credited the antifungal activity of nanoscale Ag and CuO to their antioxidative properties. Conversely, Ma et al. (2021) suggested that antifungal effects exhibited by nanoscale hydroxyapatite was due to the interplay between antioxidant and phytohormone pathways. Similar results were obtained by Noman et al. (2022) who found that F. oxysporum f. sp. Niveum infection was suppressed in watermelon treated with manganese nanoparticles by enhancing the activation of salicylic acid signaling. Alternatively, for SiO₂ NPs, Kang et al. (2021) reported a nanoscalespecific process involving the enhanced barrier deposition of silicic acid that promoted physical barrier protection in the plant cell walls against infection. The effectiveness of biochar addition on the suppression of Fusarium wilt depends on several material characteristics, including feedstock type, pyrolysis conditions, water-holding capacity, adsorption ability, nutrient content, pH, and electric conductivity (Graber et al., 2014; Iacomino et al., 2022). For example, the high nutrient content and adsorption ability of wood-derived biochar can lead to changes in the root exudate composition of tomato and watermelon, which in turn could

93

94

95

96

97

98

99

100

101

102

103

104

105

106

107

108

109

110

111

112

113

114

115

lead to increased microbiological diversity in the soil through "recruitment" of plant-beneficial bacterial species such as *Pseudomonas* (Akhter et al., 2015; Cao et al., 2017; Jin et al., 2022). Moreover, Jaiswal et al. (2022) found that the addition of biochar produced from plant waste to tomato suppresses Fusarium infection by upregulating genes coding for proteins participating in pathways involved in plant defense and phytohormone synthesis (e.g. synthesis pathways for cytokinins, auxin, jasmonic acid, brassinosteroids, and phenylpropanoids) and the downregulating of genes involved in salicylic acid synthesis. To further enhance performance of nanoparticles and biochar, they could be combined with plant growth promoting rhizobacteria (PGPR). Such combinations might activate multiple defense pathways, hense providing higher protection. PGPR have previously been used in agriculture and are known to be positively associated with plant-growth and promote plant defense against different bacterial and fungal pathogens. For example, Aydi-Ben-Abdallah et al. (2020) found that bacterial isolates naturally associated with Solanum sodomaeum and Solanum bonariense plants suppressed Fusarium wilt in tomato. This antifungal activity could be due to changes in the concentration of plant hormones such as salicylic acid and jasmonic acid (Syed Nabi et al., 2021); activation of antioxidative defense pathways (e.g. higher activity of enzymes like peroxidases, polyphenoloxidases, glucanases, chitinases, lipoxygenases, etc.) (Maciel Ferraz et al., 2014), or the direct production of antifungal compounds (Bhosale et al., 2013). For example, Azotobacter vinelandii is a bacterium with the ability to convert atmospheric nitrogen (N₂) into ammonia (NH₃) that can be used as a nitrogen source for plants (Plunkett et al., 2020). Additionally, Azotobacter vinelandii was found to synthesize antifungal compounds such as sucrose tetraamine polyphosphates that have activity under laboratory conditions and in pot experiments (Bhosale et al., 2013). Bacillus megaterium is a soil bacterium with the capacity to convert insoluble forms of

phosphorus into phosphorus-containing compounds that can be used by plants (Kang et al., 2014).
Also, Bacillus megaterium BM344-1 excretes hexadecanoic acid methyl ester and tetracosane as
part of its volatilome (Saleh et al., 2021); both compounds were shown to have antifungal activity
towards Fusarium verticillioides (Saleh et al., 2021). Furthermore, the high porosity of biochar
can provide a protective effect of bacteria located in the material pore structure. Indeed, when
adsorbed to biochar, endophytic bacteria such as Bacillus subtilis and Pseudomonas putida exhibit
a stronger effect on disease reduction than either isolate themselves or biochar on its own
(Egamberdieva et al., 2020; Chen et al., 2023). Therefore, functionalizing nanoparticles by adding
PGPR may significantly increase their potential as pesticides.
Given the known complexity of interactions between hosts, pathogens, rhizosphere microbes
(PGPR), and nanoparticles, we designed studies to compare the effect of two types of nanoparticles
(chitosan-coated mesoporous silica and nanoclay) with adsorbed PGPR and three types of biochars
(produced by pyrolysis, pyrogasification, or gasification) with adsorbed PGPR on suppression of
Fusarium wilt in tomato and watermelon. The consortium adsorbed on nanoparticles and biochar
consisted of Azotobacter vinelandii and Bacillus megaterium. This work aims to aid in
understanding the combined effect of PGPR adsorbed on nanoparticles and biochar, as well as to
elucidate mechanisms behind the suppression of Fusarium wilt in plants treated with PGPR
adsorbed on nanoparticles and biochar. Application of these treatments has the potential to provide
more sustainable and environment-friendly solutions to plant pathogen management

2. Materials and Methods

2.1. Chemicals

138	2,2-diphenyl-1-picrylhydrazyl (DPPH), 2,2'-azino-bis(3-ethylbenzothiazoline-6-sulfonic) acid
139	(ABTS), nanoclay (hydrophilic bentonite), 6-hydroxy-2,5,7,8-tetramethylchroman-2-carboxylic
140	acid (Trolox), L-ascorbic acid, tetraethylorthosilicate (TEOS), cetyltrimethylammonium bromide
141	(CTAB), and chlorotrimethylsilane were purchased from Sigma-Aldrich (St. Louis, MO, USA).
142	3-(4,5-dimethylthiazol-2-yl)-2,5-diphenyltetrazolium bromide (MTT) and Dulbecco's Modified
143	Eagle's Limiting Medium were purchased from Fisher Scientific (Waltham, MA, USA). 2-
144	[methoxy-(polyethyleneoxy) ₉₋₁₂ propyl]-trimethoxysilane was purchased from Gelest
145	(Morrisville, PA, USA). Pikovskaya medium was purchased from HiMedia Laboratories (West
146	Chester, PA, USA), while nutrient agar was purchased from Fisher Scientific (Waltham, MA,
147	USA). Chitosan was purchased from Spectrum (New Brunswick, NJ, United States). Azotobacter
148	vinelandii (strain designation: DSM 2289; ATCC 478; VKM B-1617) and Bacillus megaterium
149	(strain designation: DSM 32; VKM B-512) were purchased from ATCC (Manassas, VA, USA)
150	and kept at -80°C prior to analysis. Aries Green biochar was purchased from Aries Clean
151	Technologies LLC (Franklin, TN, USA). Naked biochar was purchased from American Biochar
152	Company (Niles, MI, USA). The remainder of the chemicals were purchased from Merck
153	Millipore (Burlington, MA, United States).
154	2.2. Synthesis and characterization of chitosan-coated mesoporous silica nanoparticles (MSN) and
155	nanoclay (NC)
156	Synthesis of chitosan-coated mesoporous silica was performed according to Buchman et al.
157	(2019), with lower ultracentrifugation speed (21,500 x g). The size of nanoparticles was
158	determined by transmission electron microscopy (TEM, HT7800 TEM, Hitachi, Japan). The pore
159	volume and surface area of MSN and NC were determined by nitrogen physisorption (Autosorb
160	IQ, Quantachrome Instruments, Boynton Beach, FL, USA). The hydrodynamic diameter and ζ

potential of the nanoparticles were determined by a Zetasizer (Nano-ZS90, Malvern Pananalytical, 161 Malvern, UK). Prior to measurements, samples were sonicated 30 min at ambient temperature. 162 The concentration of nanoparticles in samples for analyses was 0.5 mg/mL. To exclude the 163 presence of impurities in the nanoclay, elemental analysis using energy dispersive X-ray 164 spectroscopy (EDX) was done. For EDX analysis, nanoclay particles were dispersed in 95% 165 166 ethanol and mounted in a carbon-coated Ni grid. The analysis was performed with an EDX detector (80T, Oxford Instruments) attached to a Hitachi 7800 transmission electron microscope. 167 2.3. Characterization of biochars, soil substrate and fertilizer 168 Aries green biochar (AB) was derived from wood waste via downdraft gasification at the 169 temperatures averaging 450-600°C. Naked biochar (NB) was derived from recycled wood through 170 complete pyrolysis at the temperatures ranging from 550 to 900°C. A third biochar sample (named 171 "Italian biochar" – IB) was produced from wood pellets in a prototype pyrogasification system 172 <50 kW at the temperatures between 500 and 700°C (biochar is named A4 in Marmiroli et al., 173 2018). The pH and electrical conductivity (EC) measurements of the biochars was conducted 174 according to Dume (2015). In short, pH and electrical conductivity were measured in distilled 175 water at 1:10 biochar to water ratio (m/V) after shaking for 30 min. Samples were left to "settle" 176 177 10 min prior to measurements. The cation exchange capacity (CEC) was determined as described by Batista et al. (2018). Briefly, 178 2 g of sample was mixed with 100 mL of 0.5 mol/L HCl. The flask was closed and shaken at 150 179 180 rpm for 30 min at room temperature. Excess acidic aqueous solution was removed by vacuum and the material was washed twice with 50 mL of deionized water containing a few drops of 1% (m/v) 181 182 AgNO₃. Afterwards, the sample was transferred to new Erlenmeyer flask and 100 mL of 0.35 183 mol/L (CH₃COO)₂Ba was added and stirred for 15 min (room temperature). The material was

filtered and washed 3 times with 100 mL of water. The pellet was discarded, and the filtrate was titrated against 0.1 mol/L NaOH solution with phenolphthalein as indicator. The CEC was calculated using following equation:

$$CEC = \frac{V(ml) \times 0.1 \frac{mol}{l} (NaOH) \times 100}{2g}$$

188

189

190

191

192

193

194

195

196

197

198

199

200

201

202

203

204

205

206

184

185

186

The surface area and pore volume of the biochars were determined via nitrogen physisorption (Autosorb IQ, Quantachrome Instruments, Boynton Beach, FL, USA). Hydrodynamic diameter and ζ potential of biochars were determined by Zetasizer (Nano-ZS90, Malvern Pananalytical, Malvern, UK). Prior to measurements samples were sonicated 30 min at room temperature. Concentration of biochar in the samples was the same as for nanoparticles (0.5 mg/mL). Elemental analysis of biochars was determined by inductively coupled plasma optical emission spectrophotometry (ICP-OES) (iCAP 6000 series, Thermo Fisher Scientific, Waltham, MA, USA). Prior to ICP-OES analysis, 0.1 g of homogenized sample was digested with 3 mL of 68% nitric acid for 45 min at 115°C (DigiPrep MS, SCP Science, Champlain, NY, USA). The sample was diluted to 15 mL with distilled water and was allowed "settle" overnight. The content of nitrogen (N) was determined on a nitrogen analyzer (FP628, LECO, St. Joseph, MI, USA). Briefly, 0.1 g of sample was measured and closed in aluminum foil (provided with the instrument). The analytical program settings included cellulose standard, EDTA standard and an Association of American Feed Control Officials (AAFCO) standard (also provided with the instrument) that were used as negative and positive controls, respectively. As a soil substrate Promix BX (Premier Hort Tech, Quakertown, PA, USA) was used. The pH was determined according to Environmental Protection Agency (EPA) method 9045D. Briefly, a 1:1

(m/v) of substrate: distilled water was mixed for 5 min on magnetic stirrer and "left" to settle for

1h. The content of phosphorus (P) in the substrate was determined by ICP-OES (iCAP 6000 series, 207 Thermo Fisher Scientific, Waltham, MA, USA). Prior to ICP-OES analysis, samples were 208 prepared following the same procedure as for biochar. The content of N was determined with a 209 nitrogen analyzer (FP628, LECO, St. Joseph, MI, USA). Miracle-Gro all-purpose fertilizer 210 (Marysville, OH, USA) was used in the experiment. The content of P and N in the substrate was 211 212 determined using the same procedure as for soil substrate and biochar. 2.4. Adsorption of bacteria on nanoparticles and biochars, assessment of loading efficiency and 213 sample characterization 214 The adsorption of nanoparticles to the bacteria was done by according to Deng et al. (2008), with 215 some modification. In short, bacteria were first grown on nutrient agar (Fisher Scientific, Waltham, 216 MA, USA) at 28°C for 48h. Then, 2 mL of mixture containing 1 mL of 2 x10⁸ CFU/mL of A. 217 vinelandii and 1 mL 2 x108 CFU/mL B. megaterium was added in flasks containing 50 ml of 218 autoclaved distilled water and 0.1 g nanoparticles (chitosan-coated mesoporous silica or nanoclay). 219 The mixture was shaken for 6h at 6,000 rpm at ambient temperature, centrifuged at 16000 x g for 220 10 min and the recovered pellet was air-dried under a fume hood. The number of loaded bacteria 221 was determined according to Deng et al. (2018), with some modifications. One mL of supernatant 222 from the previous step was grown at nutrient agar (28°C, 48h), and the CFU/mL was determined. 223 The number of loaded bacteria was calculated by difference between initial CFU and CFU after 224 adsorption. The loading of bacteria was verified using scanning electron microscopy (SEM, 225 226 TM3030 Plus, Hitachi High-Tech Group, Japan). Sample preparation for SEM analysis included the following steps: the sample holder was cleaned with alcohol, dried and carbon tape was placed 227 228 in the middle of the holder. A small amount of powdered, homogenized sample was removed with 229 sterilized spatula, placed on carbon tape, pressed lightly with sterilized tweezers (blunt end) and

excess was taped off on filter paper. SEM images were taken at D6.1x180 in back scattered 230 electron (BSE) mode and under energy dispersive x-ray spectroscopy (EDX) observational 231 conditions. 232 For the adsorption of bacteria on biochar, the preparation of biochar was according to Husna et al. 233 (2019). Briefly, 30 g of biochar was ground and sieved to 1 mm and then autoclaved for 1h at 234 235 121°C. The loading of bacteria was verified using SEM. Inoculation of bacteria on biochar was also done as described by Husna et al. (2019). In short, 2 mL of bacterial mixture (1 mL 2 x10⁸ 236 CFU/mL of A. vinelandii and 1 mL 2 x108 CFU/ml of B. megaterium) and 11 mL of 237 distilled/autoclaved water were mixed and applied onto the biochar using a sterile syringe. Unlike 238 with nanoparticles, adsorption of bacteria to biochar is assumed to be 100 %. The biochar was 239 with bacteria was sealed in a sterile bag and left at room temperature for 24h. Sample preparation 240 and working parameters were the same as described for the nanoparticles. 241 2.5. Preparation of inoculum 242 F. oxysporum f. sp. lycopersici Race 2 and F. oxysporum f. sp. niveum were used for tomato and 243 watermelon infection, respectively. Monosporic cultures were stored at 4°C. The inoculum was 244 grown on sterile Japanese millet and ground in a mill using as described by Elmer et al. (2018). 245 246 2.6. Plant growth experimental design: Tomato (Solanum lycopersicum, cultivar Bonny Best; Totally Tomatoes, Randolph, WI, USA) 247 was grown in a first study and watermelon (Citrullus lanatus, cultivar Sweet Baby (Harris Seed 248 249 Co., Rochester, NY, USA) was used in a second experiment. Promix BX (Premier Hort Tech, Quakertown, PA, USA) soil substrate contains, according to manufacturer, 75-85% Sphagnum 250 251 peat moss, perlite, vermiculite, limestone and wetting agent. Promix's pH was 5.66 ± 0.21 ;

252	phosphorus (P) content- 562.32 ± 92.96 mg/kg and nitogen (N)- content- 0.23 ± 0.02 mg/kg (Table
253	S4; Pavlicevic et al., 2022).
254	Plants were grown from seeds in potting mix for three weeks before being transplanted into pots
255	with 250 mL of soil substrate with the various amendments. Subsequently, plants grown in non-
256	infested potting soil (controls) and potting soil infested with the fungal pathogens were grown in
257	a greenhouse in plastic pots 10 cm in diameter filled with 250 mL of potting soil. Growing
258	conditions were as follows: temperature- 25°C; light/dark period: 16h light/8h dark; relative
259	humidity during germination phase: 66%; relative humidity during growing phase: 62%. The
260	concentration of nanoparticles in soil was 250 mg/L, while the concentration of biochars in soil
261	was 100 mg/L. In both experiments, plants were infested with 0.75 g/L of millet inoculum. Mixing
262	of either nanoparticles or biochars and millet inoculum with soil was done in 2 L sterile bags. For
263	samples marked as B+F, 2 mL of bacterial mixture (1 mL 2 x10 ⁸ CFU/mL of A. vinelandii and 1
264	mL 2 x10 ⁸ CFU/mL of <i>B. megaterium</i>) was added directly into the soil, placed in a sterile bag,
265	infected with 0.75 g/L millet inoculum and mixed thoroughly by shaking. In total, there were 13
266	treatments (Table 1). The arrangement of plants was randomized, and each treatment contained 8
267	replicates.
268	Irrigation of plants was done every other day with 100 ml water per plant. Half the recommended
269	dose of Miracle-Gro (1.88 g/kg) was applied once per week (10 mL per plant). Measurements of
270	P and N content, soil pH, physiological parameters, as well as microbial analyses were performed
271	at 0, 7, 14 and 28 days after transplanting (DAT) in tomato, and 0, 10, 20, 30 DAT in watermelon.
272	2.7. Extraction and characterization of total bacteria, nitrogen-fixing bacteria and phosphorus-
273	solubilizing bacteria

274

275

276

277

278

279

280

281

282

283

284

285

286

287

288

289

290

291

292

293

294

295

296

The extraction of bacteria from the soil was performed as described by Fox et al. (2014) with some modifications. Briefly, 3 g of soil was mixed with 20 mL of sterile NaCl [0.85% (w/v)] solution for 30 min at 75 rpm at 4°C. The suspensions were then left for 1h to allow for a better separation of supernatant and soil particles. Three aliquots (0.5 mL each) were then taken: one was used for determination of nitrogen-fixing bacteria; one was used for the determination of phosphorussolubilizing bacteria and one for estimating the total number of bacteria present in the soil. These aliquots were serially diluted (by 10 fold) in 0.85% saline, and colony forming units (CFU)/mL were determined by a plate counting method. Dilution was 10⁶, and 3 plates were counted for each treatment. Bacteria were grown at 28°C for 48h. Total bacteria were grown on nutrient agar (Fisher Scientific, Waltham, MA, USA), nitrogen-fixing bacteria were grown on nitrogen-free media (NFM) (prepared according to Dobereiner et al. (1995) with 15 g of agar added per 1 L to obtain solid media) and phosphorus-solubilizing bacteria were grown on Pikovskaya agar (HiMedia Laboratories, West Chester, PA, USA). 2.8. Determination of P and N content in plant leaves Samples were dried at 105°C overnight and then ground in a coffee mill. For determination of N content, 0.1 g of dried, homogenized sample was analyzed by a N analyzer (FP628, LECO, St. Joseph, MI, USA). To determine P content, 0.1 g of homogenized sample was digested with 3 mL of 68 % nitric acid for 45 min at 115°C (DigiPrep MS, SCP Science, Champlain, NY, USA). The sample was then diluted to 15 mL with distilled water and let to "settle" overnight. P content was then determined by ICP-OES (iCAP 6000 series, Thermo Fisher Scientific, Waltham, MA, USA). 2.9. Physiological analyses Measurement of chlorophyll content was done spectrophotometrically as described by Li et al. (2018). Briefly, 0.1 g of fresh, homogenized sample was extracted with 50 mL of 95% ethanol

(120 rpm, 1h, room temperature). The pellet was discarded, and supernatant was analyzed at 649 297 and 665 nm. The content of chlorophylls was calculated according to following formulas: 298

299
$$Chl\ a\ \left(\frac{mg}{ml}\right) = \frac{(12.7 \times A665) - (2.69 \times A649)}{1000}$$

300

301
$$Chl\ b\ \left(\frac{mg}{ml}\right) = \frac{(22.9 \times A649) - (2.69 \times A665)}{1000}$$

302

306

307

308

309

310

311

312

313

314

315

316

317

318

$$Chl total = Chl a + Chl b$$

Where Chl a is chlorophyll a, Chl b is chlorophyll b, A₆₄₉ and A₆₆₅ are absorbances measured at 304 649 and 665 nm, respectively, and Chl total is total chlorophyll content. 305

The formation of radical oxygen species was monitored by the 2,2-diphenyl-1-picrylhydrazyl (DPPH) assay according to Sancez-Moreno et al. (1998). Briefly, the extraction procedure for both tests was the same: samples were air-dried for 48h under the hood and then 0.125 g of dried, homogenized sample was extracted with 6.86 mL of 70 % EtOH (120 rpm, 2h, room temperature). Then 0.1 mL of sample was mixed with 1.9 mL of fresh DPPH solution (0.025g/L DPPH in methanol), incubated for 30 min in the dark and absorbance was measured at 515 nm. As a standard, Trolox was used at 500 µmol/L, 200 µmol/L, 100 µmol/L, 50 µmol/L, 25 µmol/L and 10 umol/L. Trolox equivalents (TE) were determined from standard curves. Plant cell viability was assessed by the MTT assay as described by Shoemaker et al. (2004).

Briefly, samples were air-dried for 48h under a hood, and 0.375 g of dry, homogenized sample was extracted with 6.25 mL of distilled water at 100°C for 45 min. After the solution had cooled, 0.5 mL of sample was pipetted to a new vial. The extract was then diluted with distilled water in ratio 1:20. The MTT assay was performed by adding 400 μL of sample extract, 400 μL of 1 mM

319	ascorbic acid (in water), and 400 μL of Dulbecco's modified Eagle's medium and 120 μL MTT (3
320	mg/ml in phosphate buffered saline), followed by incubation for 60 min at 37°C. Absorbance was
321	measured at 595 nm.
322	2.10. Statistical analysis
323	All analyses were done in triplicate. A one-way analysis of variance (ANOVA) with repetition
324	was used to assess difference between samples at different time points. Differences between means
325	were determined by Tukey test at p=0.05. Testing was done in SPSS software version 24 (IBM,
326	Armonk, NY, USA). To test possible interactions between factors, a two-way ANOVA with
327	repetition was also done in XLSTAT 2016 software (Addinsoft, NY, USA).
328	
329	3. Results and Discussion:
330	3.1. Characterization of nanoparticles, biochar, soil substrate, fertilizer and samples with adsorbed
331	<u>bacteria</u>
332	All results regarding the characterization of nanoparticles, soil substrate, fertilizer, and samples
333	with the adsorbed bacteria, as well as their corresponding TEM and SEM images, are described in
334	Pavlicevic et al. (2022). Summarized here are the main findings of the material characterization.
335	Chitosan-coated mesoprous silica nanoparticles and nanoclay showed differences in all examined
336	characteristics. Chitosan-coated mesoporous silica nanoparticles (MSN) were round and with a
337	diameter of 39 ± 8 nm. Nanoclay (NC) was much larger (91 ± 7 nm) and irregular in shape. MSN
338	also had a higher surface area (87.35 m²/g) compared to NC (25.32 m²/g) and was characterized
339	by a positive ζ potential (+ 27.33 \pm 0.59 mV), while the ζ potential of NC was negative (-39.35 \pm
340	0.55 mV). These differences could be explained by the porous structure of silica nanoparticles and
341	the presence of chitosan (Pavlicevic et al., 2022).

342	Different biochar samples showed significant differences in structure, pH, EC, CEC, ratio of
343	phosphorus to nitrogen (P/N ratio) (Tables S1 and S2; Pavlicevic et al., 2022), ζ potential,
344	structure, and surface area. The "Italian" biochar (IB) had higher pH (10.62 \pm 0.03) and electric
345	conductivity (898 \pm 4.2 $\mu S/cm)$ compared to the Aries Green biochar (AB) (pH = 9.29 \pm 0.06; EC
346	= 459 \pm 2.1 $\mu S/cm)$ and the Naked biochar (NB) (pH = 9.51 \pm 0.08; EC =767 \pm 3.4 $\mu S/cm)$ (Table
347	S1). Additionally, the CEC of IB was the highest (39.1 \pm 2.8 cmol/kg), but similar to that of AB
348	$(34.7 \pm 2.9 \text{ cmol/kg})$. AB also had the lowest P/N ratio (0.05 mg/mg) , while IB had the highest
349	(3.74) (Table S2). Furthermore, ζ potential of IB was less negative (-23.6 mV) when compared to
350	AB (-26.4 mV) and NB (-27.6 mV), due to the higher content of Ca and Na in IB. However, the
351	surface area of IB was significantly lower (13.11 m^2/g) than those of AB (59.54 m^2/g) and NB
352	(42.73 m²/g). Structures of biochars were also different (Pavlicevic et al., 2022): IB had more
353	regular structure compared to AB, while the structure of NB was similar to a honeycomb with
354	highly macroporous surface (Figure S1). Given that all biochars were produced from same
355	feedstock material, these differences reflect the different conditions (most of all, temperature)
356	under which biochars were produced.
357	The ratio of individual bacteria species adsorbed to biochars and nanoparticles adsorbed to bacteria
358	was relatively similar between materials and close to a 1:1 ratio (Pavlicevic et al., 2022). However,
359	the distribution of the bacteria on biochar showed some differences: bacteria were located farther
360	from the surface and were more uniformly distributed in AB and NB, whereas in the IB they were
361	more clustered and closer to the surface of biochar (Figure S2; Pavlicevic et al., 2022).
362	3.2. Chlorophyll content
363	As evident from Figure 1, treated plants had higher chlorophyll content compared to control plants
364	infected with Fusarium. However, in both tomato (Fig. 1A) and watermelon experiments (Fig.

365

366

367

368

369

370

371

372

373

374

375

376

377

378

379

380

381

382

383

384

385

386

387

1B), the biggest increase was observed in plants treated with biochar and nanoparticles codelivered with bacteria. For example, in the tomato experiment (Fig. 1A), the addition of chitosancoated mesoporous silica nanoparticles adsorbed onto bacteria (MSN + B + F) increased chlorophyll content in infected plants 1.62 times compared to chitosan-coated mesoporous silica nanoparticles added alone (MSN + F) (1.11 times). Such differences were likely due to the combined effect of nanoparticles (or biochars) and the documented antifungal effect of Azotobacter vinelandii and Bacillus megaterium (Bhosale et al., 2013; Saleh et al., 2021). However, watermelon showed overall greater responsiveness to treatment compared to tomato (Fig. 1B), although this could also be due to the fact that infection in watermelon was less severe. Similar to tomato, the greatest influence on chlorophyll content in the infected watermelon plants was exhibited by chitosan-coated mesoporous silica nanoparticles with bacteria (MSN+B+F). These findings may corroborate the hypothesis of Kang et al. (2021), who suggested that the mesoporous silica nanoparticles stimulate the formation of an enhanced protective layer in the roots that diminishes the impact of infection. This hypothesis could also explain why the MSN treatment was more efficient compared to the NC treatment. The addition of MSN increased chlorophyll content in infected tomato plants 1.12 times and infected watermelon plants 1.63 times; NC increased the content of chlorophyll in infected tomato plants 1.10 times and in infected watermelon plants 1.38 times. However, it is also possible that the effect of mesoporous silica nanoparticles was enhanced by the addition of chitosan and its known antifungal effect (Carmona et al., 2021). Additionally, larger effect of both MSN and NC on watermelon compared to tomato could be due to the fact that watermelon belong to Cucurbitaceae family and thus needs more Si compared to tomato. Similar to the nanoparticles, the addition of the bacterial consortium to biochar had a positive effect on chlorophyll content, but to a lesser extent (Fig. 1). In agreement

with our previous results, the response of watermelon and tomato to biochar addition was species-specific. For example, the presence of "Italian" biochar with infected watermelon (IB+F) increased the chlorophyll content 1.08 times, while the addition of "Italian" biochar with adsorbed bacteria (IB+B+F) increased chlorophyll content 1.22 times (Fig. 1B). The most efficient biochar with tomato was Aries biochar (Fig. 1A). Specifically, the addition of Aries biochar to infected tomato (AB+F) increased chlorophyll content 1.23 times compared to 1.35 times with Aries biochar with adsorbed bacteria was added (AB+B+F) (Fig. 1A). The prominent effect of AB on disease suppression is likely a consequence of production temperature. AB was produced by gasification that is characterized by lower temperatures compared to pyrolysis and pyrogasification; Iacomino et al. (2022) found that biochars produced in mid-temperature range (350-600°C) showed a more prominent effect on disease suppression compared to those produced at low or high temperatures. The same findings could be used to explain why the effect of IB was more effective than NB, since IB was produced by pyrogasification, e.g. under lower temperatures than NB (which was the product of pyrolysis).

3.3. Nitrogen content in leaves

The results of N content in the leaves of tomato and watermelon plants are given in Table 2. Greater N content in diseased plants (F) compared to healthy control plants (C) was evident; these findings align with Domínguez et al. (2016), Bi et al. (2022), and Orr et al. (2022). Higher N content in infected plants can be the result of the upregulation of genes involved in N metabolism (Orr et al., 2022). While Domínguez et al. (2016), Bi et al. (2022) and Orr et al. (2022) all reported a positive correlation between disease severity and N content, Hoffland et al. (2000) found that a connection between disease severity and N content was strongly dependent on the type of pathogen. Our results also suggest that the host plant species can also determine the response to a particular

treatment. Although N content in infected tomato and watermelon plants at the end of experiments
was similar (51.4±2.9 mg/g and 50.7±4.8 mg/g, respectively), the same treatments had different
effects in the two species. For example, NC-treated infected plants (NC+F) had lower N content
compared to MSN treated plants (MSN+F) in tomato, but the situation was reversed in watermelon
(Table 2). However, when the same samples had bacteria adsorbed, the response was reversed (e.g.
MSN+B+F had lower N content in tomato and higher in watermelon when compared to NC+B+F).
These findings may be explained by the fact that although disease could increase N content and in
turn change the composition of the microbial community (Bi et al., 2022), changes in rhizobia
composition caused by the introduction of the consortium were more impactful.
The impact of individual biochars and biochars with adsorbed bacteria on disease suppression in
tomato and watermelon was also different (Table 2). In tomato, the lowest N content was detected
in AB+F (34.0±2.9 mg/g) and AB+B+F (47.6±3.6 mg/g). Although watermelon AB+F treatment
had the lowest N content with the biochars, the greatest content was the NB biochar with adsorbed
bacteria (sample NB+B+F) (Table 2). The possible reason for the higher efficacy of AB compared
to IB and NB could be the greater N content in AB (7.5 \pm 0.6 mg/g) compared to IB (5.8 \pm 0.2
mg/g) and NB (3.9 ± 0.4 mg/g) (Pavlicevic et al., 2022). Biochars with a higher nutrient content
have been shown to be more prone to "recruit" beneficial fungi and bacteria that could alleviate
infection symptoms (Akhter et al., 2015; Cao et al., 2017; Jin et al., 2022). As noted above, NB
was produced by pyrolysis and has a highly porous structure (Pavlicevic et al., 2022). These
characteristics are known to be important for wood-derived biochars to ensure longer "life" of
adsorbed bacteria and therefore, promotes more beneficial changes in rhizobia activity (Akhter et
al., 2016; Chen et al., 2023).

3.4.Phosphorus content in leaves

At the final harvest, the phosphorus content in the leaves of <i>Fusarium</i> infected plants was 3.33-
times (tomato) and 3.65-times (watermelon) higher compared to non-infected (control) plants
(Table 3). These results are in accordance with Ma et al. (2021) who reported an increase in P
content of approximately 2.5-times in diseased plants compared to healthy tomato plants. Higher
P content in diseased plants could be explained by Fusarium-induced up-regulation of genes such
as the betaine lipid synthase 1 (BTA1), which yields phosphorus-free membrane lipids that enable
the infection to spread inside the cells (Zhang et al., 2016). Given that production of membrane
void of phosphorus-containing lipid is required for "successful" infection (Zhang et al., 2016), less
phosphorus is "spent" in synthetic pathways and thus, final content of phosphorus is higher in
diseased plants compared to healthy ones. Hagerty et al. (2021) reported that P content was not
correlated with the severity of disease in wheat, whereas El-Shennawy et al. (2010) found that an
increase in P content reduced the incidence of Fusarium infection in chickpea (Cicer arietinum),
lupine (Lupinus sp.), and lentil (Lens culinaris). However, Jastrzębska et al. (2020) reported that
not only the content but also the source of phosphorus was important; specifically, fertilizers
prepared from organic residues and/or activated with bacteria showed a more pronounced
antifungal effect compared to the commercial products. In tomato, the greatest difference in P
content between treated and diseased plants was observed for B+F and IB+B+F (Table 3). In
watermelon, the highest P content was detected in the AB+B+F treatment. These results suggest
that the incorporation of PGPR led to the changes in the microbial community that modified the
response of plants to Fusarium infection; these findings align with that of Syed Nabi et al. (2021),
Delgado-Ramírez et al. (2021), and Zhou et al. (2022).

3.5. Plant cell viability

Metabolically active cells have intact membranes and contain a variety of compounds that are intermediates of Krebs cycles (such as malate, glutamate, succinate, etc.) that can reduce MTT to formazan (Liu et al., 1997). In both tomato and watermelon, all treatments (except in tomato with nanoclay) increased viability (Figure 2 and Figure 3). This is in agreement with Alvarez-Carvajal et al. (2020) who reported that chitosan-coated silver nanoparticles increased viability in tomato and Chouhan et al. (2022) who found that a nickel chitosan nanoconjugate had a positive effect on the viability in Fusarium-infected wheat. However, the difference in the response of tomato and watermelon was again evident. In tomato, MSN-containing treatments had more impact on viability (an increase of 1.37-fold for MSN+F and 1.43-fold for MSN+B+F) than did NCcontaining treatments (Fig. 2A). This is also evident from Figure 3; in the nanoparticle only treatments, MSN treatment had a greater impact on disease suppression than did NC (Fig. 3B and 3C). In watermelon, the situation was reversed: in NC-treated plants, viability was increased 1.54 times (for NC+F samples) and 1.92 times (for NC+B+F). For MSN-treated plants, the increase was more modest; 1.45 times for MSN+F samples and 1.70 times for MSN+B+F (Fig. 2B). However, in both species the most effective biochar-containing sample was AB+B+F (Fig. 3D), increasing viability in diseased tomato and watermelon by 1.51 and 2.43 times, respectively. This is in accordance with the chlorophyll content results and could be explained by the joint effect of lower temperature during gasification (Iacomino et al., 2022) and the presence of plant-growth promoting rhizobacteria (Egamberdieva et al., 2020). Additionally, all treatments in which bacteria were present (including treatments where bacteria were added directly into the soil) increased viability compared to corresponding treatments without bacteria (Fig. 2, Fig. 3). This provides additional evidence of the pivotal role of rhizobacteria in plant's defense.

3.6.Antioxidant properties

456

457

458

459

460

461

462

463

464

465

466

467

468

469

470

471

472

473

474

475

476

477

479

480

481

482

483

484

485

486

487

488

489

490

491

492

493

494

495

496

497

498

499

500

501

As evident in Figure 4, all treatments increased the content of antioxidant compounds in diseased tomato and watermelon. These findings agree with Buchman et al. (2019) and Ma et al. (2021), who found that nanoparticle treatment increased the expression of stress-related genes and the activity of antioxidative enzymes in watermelon and tomato, respectively. Such an increase in antioxidative compounds is a defense against oxidative stress induced by Fusarium infection (Mandal et al., 2008). However, similar to chlorophyll content and viability results above, diseased tomato and watermelon responded differently to equivalent treatments. For example, MSN increased the content of antioxidant compounds in tomato by 4.27% (Fig. 4A), while the increase in watermelon was 33.78% (Fig. 4B). Conversely, nanoclay was less efficient in watermelon compared to MSN (antioxidant compound content was 29.16% higher than in *Fusarium* control) (Fig. 4B), but the antioxidant capacity in tomato increased 170% following the NC treatment (Fig.4A). Both nanoclay and chitosan-coated mesoporous silica nanoparticles contain silicon (Si), and Si has been shown to alleviate damage of Fusarium infection by activating antioxidant response (Huang et al., 2011). The most effective biochar in both watermelon and tomato was NB, likely due to its high porosity. With exception of NB+B+F in tomato, all treatments with adsorbed bacteria had a more pronounced effect on antioxidant capacity compared to corresponding bacteria-free treatments. For example, the content of antioxidant compounds in the diseased tomato increased by 208% after AB addition, whereas the increase with AB+B was 367%. Also, the addition of bacteria directly into the soil of infected plants increased the content of antioxidant compounds in tomato and watermelon by 19.84 and 27.77%, respectively. This aligns Zibanezhadian et al. (2020) who found that addition of Bacillus thuringiensis to Fusarium-infected tomato plants increased the expression of superoxide dismutase, catalase, and glutathione Stransferase genes.

As evident from Table 4 (procedure described in supplementary material), no statistically

3.7.Soil pH and microbiological analysis

502

503

504

505

506

507

508

509

510

511

512

513

514

515

516

517

518

519

520

521

522

523

524

significant differences were found in soil pH between diseased and treated plants of either species at harvest. Such results may be a function of the buffering capacity of biochar (Shi et al., 2017), although additional work is needed to confirm that hypothesis. As evident from Figure 5, the total extractable bacteria content in the soil of infected controls of both species was lower than the healthy control. This decrease in total extractable bacteria may imply competitiveness between Fusarium and rhizobacteria species (Zhang et al., 2022; Jaiwal et al., 2022). However, the number of nitrogen-fixing bacteria in infected control plants in both species was greater than healthy controls (Figure 6); this increase could be a consequence of Fusarium-mediated "requirement" of beneficial entophytic bacteria (Yuan et al., 2022). The same explanation could also apply to the increased content of phosphorus-solubilizing bacteria in Fusarium-infected tomato compared to healthy controls (Figure 7A). However, this was not true for watermelon, which exhibited reduced content of P-solubilizing bacteria in the soil of infected plants compared to healthy controls (Figure 7B). Furthermore, the effects of equivalent treatments in tomato and watermelon were widely different. For example, the largest increase of total bacteria content in tomato was with NC+B and IB+B (Fig. 5A); in watermelon, MSN and the direct addition of bacteria to the soil had the greatest impact (Fig. 5B). The addition of chitosan-coated mesoporous silica nanoparticles also led to the greatest content of N-fixing bacteria in the soil of diseased tomato (Fig. 6A), whereas for watermelon, IB yielded the greatest content of N-fixing bacteria (Fig. 6B). IB+B treatment showed the biggest impact on the content on P-solubilizing bacteria in tomato (Fig. 7A), while NC gave the largest increase in content of P-solubilizing bacteria in the soil of infected watermelon. As Merino et al. (2018), Buchman et al. (2019) and

Aseel et al. (2022) showed both NC and MSN were shown to exhibit antimicrobial effects through the upregulation of genes involved in plant defense and the activation of antioxidative enzymes. Further experiments are needed to characterize changes in rhizobia composition in tomato and watermelon as a function of disease and treatment and to elucidate the underlying mechanisms driving species-specific responses.

4. Conclusion

Azotobacter vinelandii and Bacillus megaterium adsorbed on chitosan-coated mesoporous silica nanoparticles, nanoclay, and biochars alleviated the damage from Fusarium wilt in both tomato and watermelon. Although different treatments impacted disease progression in watermelon and tomato to a different extent, all treatments increased the content of chlorophyll and antioxidative compounds. The content of total-, nitrogen-fixing- and phosphorus-solubilizing bacteria varied both as a consequence of treatments and plant species, which likely is a consequence of different rhizobial composition in tomato and watermelon. Treatment with adsorbed bacteria showed a greater positive effect on all measured endpoints, which implies an additive impact of the microbial consortium and nanoparticles (or biochar) on disease suppression. These findings increase our understanding of the potential additive positive effects of novel nanoscale-based formulations of biopesticides as a sustainable disease management strategy.

5. Conflict of Interest

The authors declare that the research was conducted in the absence of any commercial or financial relationships that could be construed as a potential conflict of interest.

6. Author Contributions

Authors MP, WE, EM and NM conceived experimental design. Authors MP, WE, NZM, WA and RP performed experimental analysis and read original draft. Author MP performed statistical

analysis	and wrote original draft. Authors WE, NZM, CD, TOK, CLH, EM, LP, MM, MC, NM
and JW l	nelped with experiment design, analyzed and discussed data, and helped to write the final
manuscri	ipt.
7	. Funding
Funding	for this research was provided by the project "Go for IT" financed by Fondazione CRUI
This mat	terial is based upon work supported by the National Science Foundation under Grant No.
CHE-200	01611, the NSF Center for Sustainable Nanotechnology (CSN). The CSN is part of the
Centers	for Chemical Innovation Program. This work has benefited from the equipment and
framewo	ork of the COMP-HUB Initiative, funded by the "Departments of Excellence" program of
the Italia	n Ministry for Education, University and Research (MIUR, 2018–2022).
8. Suppl	ementary Material:
Determin	nation of soil pH after treatment: The soil pH was determined after harvest using the
same pro	ocedure as for the soil substrate. In short, 1:1 (m/v) of substrate: distilled water was
mixed fo	or 5 min on magnetic stirrer and "left" to settle for 1h before measurement.
Figure S	1: Representative scanning electron microscopy (SEM) images of biochars. A- "Italian"
biochar;	B- Aries Green biochar; C-Naked biochar.
Figure S	22: Representative scanning electron microscopy (SEM) images of nanoparticles and
biochars	with adsorbed bacteria. A-mesoporous silica + bacteria; B- nanoclay + bacteria; C-
"Italian"	biochar + bacteria; D- Aries Green biochar + bacteria; E-Naked biochar + bacteria.
Table S1	: pH, conductivity and cation exchange capacity (CEC) of biochars.
T	Table S2: Content of phosphorus (P) and nitrogen (N) in biochars. References:
Abo-Ely	ousr, K.A.M., Al-Qurashi, A.D., Saad, M., Ibrahim, O.H.M., Mousa, M.A.A, 2022
Efficacy	of Azadirachta indica and Punica granatum extracts in the control of Cuminum cyminum

- 571 wilt disease caused by Fusarium oxysporum f. sp. cumini. Sustainability 14, 15233.
- 572 <u>https://doi.org/10.3390/su142215233</u>
- Adisa, I.O., Reddy Pullagurala, V.L., Rawat, S., Hernandez-Viezcas, J.A., Dimkpa, C.O., Elmer,
- W.H., White, J.C., Peralta-Videa, J.R., Gardea-Torresdey, J.L., 2018. Role of cerium compounds
- 575 in Fusarium wilt suppression and growth enhancement in tomato (Solanum lycopersicum). J.
- 576 Agric. Food Chem. 66, 5959–5970. https://doi.org/10.1021/acs.jafc.8b01345
- 577 Ahmad, M., Ali, A., Ullah, Z., Sher, H., Dai, D.Q., Ali, M., Iqbal, J., Zahoor, M., Ali, I., 2022.
- 578 Biosynthesized silver nanoparticles using Polygonatum geminiflorum efficiently control fusarium
- 579 wilt disease of tomato. Front Bioeng Biotechnol. 10, 988607.
- 580 https://doi.org/10.3389/fbioe.2022.988607
- Ahmed, I.S.A., Yadav, D.R., Lee, Y.S., 2016. Applications of nickel nanoparticles for control of
- Fusarium wilt on lettuce and tomato. Int. J. Innov. Res. Technol. Sci. Eng. 5, 7378–7385.
- 583 <u>https://doi.org/10.15680/IJIRSET.2016.0505132</u>
- Ain, Q.U., Asad, S., Ahad, K., Safdar, M.N., Jamal, A., 2022. Antimicrobial activity of Pinus
- wallachiana leaf extracts against Fusarium oxysporum f. sp. cubense and analysis of its fractions
- by HPLC. Pathogens. 11, 347. https://doi.org/10.3390/pathogens11030347
- 587 Akhter, A., Hage-Ahmed, K., Soja, G., Steinkellner, S., 2015. Compost and biochar alter
- 588 mycorrhization, tomato root exudation, and development of Fusarium oxysporum f. sp.
- 589 lycopersici. Front Plant Sci. 6, 529. https://doi.org/10.3389/fpls.2015.00529
- 590 Alvarez-Carvajal, F., Gonzalez-Soto, T., Armenta-Calderón, A.D., Méndez Ibarra, R., Esquer-
- Miranda, E., Juarez, J., Encinas-Basurto, D., 2020. Silver nanoparticles coated with chitosan
- 592 against Fusarium oxysporum causing the tomato wilt. Biotecnia 22, 1-15.
- 593 https://doi.org/10.18633/biotecnia.v22i3.952

- Aseel, D.G., Abdelkhalek, A., Alotibi, F.O., Samy, M.A., Al-Askar, A.A., Arishi, A.A., Hafez,
- 595 E.E., 2022. Foliar application of nanoclay promotes potato (Solanum tuberosum L.) growth and
- 596 induces systemic resistance against potato virus Y. Viruses. 14, 2151.
- 597 <u>https://doi.org/10.3390/v14102151</u>
- 598 Aydi-Ben-Abdallah, R., Jabnoun-Khiareddine, H., Daami-Remadi, M., 2020. Fusarium wilt
- biocontrol and tomato growth stimulation, using endophytic bacteria naturally associated with
- 600 Solanum sodomaeum and S. bonariense plants. Egypt. J. Biol. Pest Control 30, 113.
- 601 <u>https://doi.org/10.1186/s41938-020-00313-1</u>
- Batista, E.M.C.C., Shultz, J., Matos, T.T.S, Fornari, M.R., Ferreira, T.M., Szpoganicz, B., de
- Freitas, R.A., Mangrich, A.S., 2018. Effect of surface and porosity of biochar on water holding
- 604 capacity aiming indirectly at preservation of the Amazon biome. Sci. Rep. 8, 10677.
- 605 <u>https://doi.org/10.1038/s41598-018-28794-z</u>
- Bhosale, H.J., Kadam, T.A., Bobade, A.R., 2013. Identification and production of Azotobacter
- 607 vinelandii and its antifungal activity against Fusarium oxysporum. J. Environ. Biol. 34, 177-182.
- Bi, J., Song, A., Li, S., Chen, M., Wang, Y., Wang, S., Si, Z., Wang, E., Zhang, J., Asante-Badu,
- B., Njyenawe, M.C., Zhang, Q., Xue, P., Fan, F., 2022. Plant physiology, microbial community,
- and risks of multiple fungal diseases along a soil nitrogen gradient. Appl. Soil Ecol. 175, 104445.
- 611 https://doi.org/10.1016/j.apsoil.2022.104445
- Buchman, J.T., Elmer, W.H., Ma, C., Landy, K.M., White, J.C., Haynes, C.L., 2019. Chitosan-
- 613 coated mesoporous silica nanoparticle treatment of Citrullus lanatus (watermelon): enhanced
- fungal disease suppression and modulated expression of stress-related genes. ACS Sustainable
- 615 Chem. Eng. 7,19649–19659. https://doi.org/10.1021/acssuschemeng.9b04800

- 616 Cai, H., Tao, N., Guo, C., 2020. Systematic investigation of the effects of macro-elements and iron
- on soybean plant response to Fusarium oxysporum infection. Plant Pathol. J. 36, 398-405.
- 618 <u>https://doi.org/10.5423/PPJ.OA.04.2020.0069</u>
- 619 Cao, Y., Ma, Y., Guo, D., Wang, Q., Wang, G., 2017. Chemical properties and microbial responses
- 620 to biochar and compost amendments in the soil under continuous watermelon cropping. Plant Soil
- 621 Environ. 63, 1-7. https://doi.org/10.17221/141/2016-PSE
- 622 Carmona, S.L., Villarreal-Navarrete, A., Burbano-David, D., Gómez-Marroquín, M., Torres-
- Rojas, E., Soto-Suárez, M., 2021. Protection of tomato plants against *Fusarium oxysporum* f. sp.
- 624 lycopersici induced by chitosan. Revista colombiana de ciencias horticolas 15, e12822.
- 625 https://doi.org/10.17584/rcch.2021v15i3.12822
- 626 Chen, W., Wu, Z., Liu, C., Zhang, Z., Liu, X., 2023. Biochar combined with Bacillus subtilis SL-
- 44 as an eco-friendly strategy to improve soil fertility, reduce Fusarium wilt, and promote radish
- 628 growth. Ecotoxicol Environ Saf. 251, 114509. https://doi.org/10.1016/j.ecoenv.2023.114509
- 629 Chouhan, D., Dutta, A., Kumar, A. Mandal, P., Choudhuri, C., 2022. Application of nickel
- chitosan nanoconjugate as an antifungal agent for combating Fusarium rot of wheat. Sci. Rep. 12,
- 631 14518. https://doi.org/10.1038/s41598-022-18670-2
- 632 Delgado-Ramírez, C.S., Hernández-Martínez, R., Sepúlveda, E., 2021. Rhizobacteria associated
- with a native Solanaceae promote plant growth and decrease the effects of Fusarium oxysporum
- 634 in tomato. Agronomy 11, 579. https://doi.org/10.3390/agronomy11030579
- Deng, S., Upadhyayula, V.K.K., Smith, G.B., Mitchell, M.C., 2008. Adsorption equilibrium and
- kinetics of microorganisms on single-wall carbon nanotubes. IEEE Sensors Journal 8, 954-962.
- 637 https://doi.org/10.1109/JSEN.2008.923929

- Dobereiner, J., Urquiaga, S., Boddey, R.M., 1995. Alternatives for nitrogen nutrition of crops in
- 639 tropical agriculture. In: Ahmad, N. (eds) Nitrogen economy in tropical Soils. Developments in
- Plant and Soil Sciences, vol 69. Springer, Dordrecht. https://doi.org/10.1007/978-94-009-1706-
- 641 4 32
- Domínguez, S., Rubio, M.B., Cardoza, R.E., Gutiérrez, S., Nicolás, C., Bettiol, W., Hermosa, R.,
- Monte, E., 2016. Nitrogen metabolism and growth enhancement in tomato plants challenged with
- 644 Trichoderma harzianum expressing the Aspergillus nidulans acetamidase amdS gene. Front
- 645 Microbiol. 7, 1182. https://doi.org/10.3389/fmicb.2016.01182
- Dongzhen, F., Xilin, L., Xiaorong, C., Wenwu, Y., Yunlu, H., Yi, C., Jia, C., Zhimin, L., Litao,
- 647 G., Tuhong, W., Xu, J., Chunsheng, G., 2020. Fusarium species and Fusarium oxysporum species
- 648 complex genotypes associated with yam wilt in south-central China. Front Microbiol. 11, 1964.
- 649 <u>https://doi.org/10.3389/fmicb.2020.01964</u>
- Dume, B., 2015. Characterization of biochar produced at different temperatures and its effect on
- 651 acidic Nitosol of Jimma, southwest Ethiopia. Int. J. Soil Sci. 10, 63-73.
- 652 <u>https://doi.org/10.3923/ijss.2015.63.73</u>
- Egamberdieva, D., Shurigin, V., Alaylar, B., Ma, H., Müller, M.E.H., Wirth, S., Reckling, M.,
- Bellingrath-Kimura, S.D., 2020. The effect of biochars and endophytic bacteria on growth and
- root rot disease incidence of Fusarium infested narrow-leafed lupin (Lupinus angustifolius L.).
- Microorganisms. 8, 496. https://doi.org/10.3390/microorganisms8040496
- Elmer, W., De La Torre-Roche, R., Pagano, L., Majumdar, S., Zuverza-Mena, N., Dimkpa, C.,
- 658 Gardea-Torresdey, J., White, J. C., 2018. Effect of metalloid and metal oxide nanoparticles on
- 659 Fusarim Wilt of watermelon. Plant Dis. 102, 1394–1401. https://doi.org/10.1094/PDIS-10-17-
- 660 1621-RE

- 661 El-Shennawy, R.Z., Omran, M.M., Abd El-Motteleb, F.A., 2010. Effect of phosphorus fertilizer
- treatments on incidence of Fusarium root-rot/wiltdisease complex, and on yield components of
- 663 lupine, chickpea and lentil crops. Arab Univ. J. Agric. Sci. 18, 193-202.
- 664 <u>https://doi.org/10.21608/ajs.2010.14989</u>
- Epstein, L., Kaur, S., Henry, P.M., 2022. The emergence of Fusarium oxysporum f. sp. apii Race
- 4 and Fusarium oxysporum f. sp. coriandrii highlights major obstacles facing agricultural
- production in coastal california in a warming climate: a case study. Front. Plant Sci. 13, 921516.
- 668 https://doi.org/10.3389/fpls.2022.921516
- 669 Fox, A., Kwapinski, W., Griffiths, B.S., and Schmalenberger, A., 2014. The role of sulfur- and
- 670 phosphorus-mobilizing bacteria in biochar-induced growth promotion of Lolium perenne. FEMS
- 671 Microbiol. Ecol. 90, 78-91. https://doi.org/10.1111/1574-6941.12374
- Figueiredo Silva, F., Kaplan, S., Tobar, F. A. M., Potts, M. D., Martinez, R. L. E., Zilberman, D.,
- 673 2023. Estimating worldwide benefits from improved bananas resistant to Fusarium wilt tropical
- 674 race 4. J. Agric. Appl. Econ., 1–15. https://doi.org/10.1002/jaa2.41Graber, E.R., Frenkel, O.,
- Jaiswal A.K., Elad Y., 2014. How may biochar influence severity of diseases caused by soilborne
- pathogens? Carbon Manag. 5(2), 169–183. https://doi.org/10.1080/17583004.2014.913360
- 677 González-Domínguez, E., Meriggi, P., Ruggeri, M., Rossi, V., 2021. Efficacy of fungicides against
- Fusarium head blight depends on the timing relative to infection rather than on wheat growth stage.
- 679 Agronomy 11, 1549. https://doi.org/10.3390/agronomy11081549
- Hagerty, C. H., McLaughlin, K. R., Kroese, D. R., Lutcher, L. K., 2021. Phosphorus supply does
- 681 not affect Fusarium crown rot of winter wheat. PhytoFrontiers 1, 354-358.
- 682 https://doi.org/10.1094/PHYTOFR-01-21-0010-R

- Havrlentová, M., Šliková, S., Gregusová, V., Kovácsová, B., Lancaricová, A., Nemecek, P.,
- Hendrichová, J., Hozlár, P., 2021. The Influence of artificial Fusarium infection on oat grain
- quality. Microorganisms 9, 2108. https://doi.org/10.3390/microorganisms9102108
- Hoffland, E., Jeger, M.J., van Beusichem, M.L., 2000. Effect of nitrogen supply rate on disease
- resistance in tomato depends on the pathogen. Plant and Soil 218, 239-247
- 688 https://doi.org/10.1023/A:1014960507981
- Huang, C-H., Roberts, P.D., Datnoff, L.E., 2011. Silicon suppresses Fusarium crown and root rot
- of tomato. J. Phytopathol. 159, 546 554. https://doi.org/10.1111/j.1439-0434.2011.01803.x
- Husna, N., Budianta, D., Munandar, M., Napoleon, A., 2019. Evaluation of several biochar types
- as inoculant carrier for indigenous phosphate solubilizing microoorganism from acid sulphate soil.
- 693 J. Ecol. Eng. 20, 1–8. https://doi.org/10.12911/22998993/109078
- Iacomino, G., Idbella, M., Laudonia, S., Vinale, F., Bonanomi, G., 2022. The suppressive effects
- of biochar on above- and belowground plant pathogens and pests: a review. Plants 11, 3144.
- 696 https://doi.org/10.3390/plants11223144
- Jaiswal, A.K., Alkan, N., Elad, Y., Sela, N., Philosoph, A.M., Graber, E.R., Frenkel O., 2020.
- 698 Molecular insights into biochar-mediated plant growth promotion and systemic resistance in
- 699 tomato against Fusarium crown and root rot disease. Sci Rep. 10, 13934.
- 700 https://doi.org/10.1038/s41598-020-70882-6
- Jamil, F.N., Hashim, A.M., Yusof, M.T., Saidi, N.B., 2022. Analysis of soil bacterial communities
- and physicochemical properties associated with Fusarium wilt disease of banana in Malaysia. Sci
- 703 Rep. 12, 999. https://doi.org/10.1038/s41598-022-04886-9

- Jastrzębska, M., Wachowska, U., Kostrzewska, M.K., 2020. Pathogenic and non-pathogenic
- fungal communities in wheat grain as influenced by recycled phosphorus fertilizers: a case study.
- 706 Agriculture 10, 239. https://doi.org/10.3390/agriculture10060239
- 707 Jin, X., Bai, Y., u Rahman, M. K., Kang, X., Pan, K., Wu, F., Pommier, T., Zhou, X., Wei, Z.,
- 708 2022. Biochar stimulates tomato roots to recruit a bacterial assemblage contributing to disease
- resistance against Fusarium wilt. iMeta 1(3), e37. https://doi.org/10.1002/imt2.37
- Kang, H., Elmer, W., Shen, Y., Zuverza-Mena, N., Ma, C., Botella, P., White, J.C., Haynes, C.L.,
- 711 2021. Silica nanoparticle dissolution rate controls the suppression of *Fusarium* wilt of watermelon
- 712 (Citrullus lanatus). Environ. Sci. Technol. 55, 13513–13522.
- 713 https://doi.org/10.1021/acs.est.0c07126
- 714 Kang, S.M., Radhakrishnan, R., You, Y.H., Joo, G.J., Lee, I.J., Lee, K.E., Kim, J.H., 2014.
- 715 Phosphate solubilizing Bacillus megaterium mj1212 regulates endogenous plant carbohydrates
- and amino acids contents to promote mustard plant growth. Indian J. Microbiol. 54, 427–443.
- 717 https://doi.org/10.1007/s12088-014-0476-6
- Katiyar, D., Hemantaranjan, A., Singh, B., 2015. Chitosan as a promising natural compound to
- 719 enhance potential physiological responses in plant: a review. Ind. J. Plant Physiology, 1-9.
- 720 <u>https://doi.org/10.1007/s40502-015-0139-6</u>
- 721 Li, Y., Liu, C., Zhang, J., Yang, H., Xu, L., Wang, Q., Sack, L., Wu, X., Hou, J., He, N., 2018.
- Variation in leaf chlorophyll concentration from tropical to cold-temperate forests: Association
- 723 with gross primary productivity, Ecol. Indic. 85, 383-389.
- 724 https://doi.org/10.1016/j.ecolind.2017.10.025

- Lin, W., Lin, M., Zhou, H., Wu, H., Li, Z., Lin, W., 2018. The effects of chemical and organic
- 726 fertilizer usage on rhizosphere soil in tea orchards. PLoS One 14, e0217018.
- 727 <u>https://doi.org/10.1371/journal.pone.0217018</u>
- Liu, Y., Peterson, D.A., Kimura, H., Schubert, D., 1997. Mechanism of cellular 3-(4,5-
- dimethylthiazol-2-yl)-2,5-diphenyltetrazolium bromide (MTT) reduction. J Neurochem. 69, 581-
- 730 593. https://doi.org/10.1046/j.1471-4159.1997.69020581.x
- Lopez-Lima, D., Mtz-Enriquez, A.I. Carrión, G., Basurto-Cereceda, S., Pariona, N., 2021. The
- bifunctional role of copper nanoparticles in tomato: effective treatment for Fusarium wilt and plant
- 733 growth promoter. Scientia Horticulturae 277, 109810.
- 734 https://doi.org/10.1016/j.scienta.2020.109810
- Ma, C., Li, Q., Jia, W., Shang, H., Zhao, J., Hao, Y., Li, C., Tomko, M., Zuverza-Mena, N., Elmer,
- 736 W., White, J.C., Xing, B., 2021. Role of nanoscale hydroxyapatite in disease suppression of
- 737 Fusarium-infected tomato. Environ Sci Technol. 55(20), 13465-13476.
- 738 https://doi.org/10.1021/acs.est.1c00901
- Maciel Ferraz, H. G, Sousa Resende, R., Ricardino Silveira, P., Lage Andrade, C.C., Aparecida
- Milagres, E., Rogério Oliveira, J., de Ávila Rodrigues, F., 2014. Rhizobacteria induces resistance
- against Fusarium wilt of tomato by increasing the activity of defense. Bragantia 73, 274-283.
- 742 https://doi.org/10.1590/1678-4499.0124
- Mahmood, I., Imadi, S.R., Shazadi, K., Gul, A., Hakeem, K.R., 2016. Effects of pesticides on
- environment. In: Hakeem KR, Akhtar MS, Abdullah SNA (eds) Plant, Soil and Microbes, vol 1.
- 745 Implications in Crop Science. Springer International Publishing, Cham, pp 253–269.

- Mandal, S., Mitra, A., Mallick, N., 2008. Biochemical characterization of oxidative burst during
- 747 interaction between *Solanum lycopersicum* and *Fusarium oxysporum* f. sp. Lycopersici. Physiol.
- Mol. Plant Pathol. 72, 56-61. https://doi.org/10.1016/j.pmpp.2008.04.002
- Marmiroli, M., Bonas, U., Imperiale, D., Lencioni, G., Mussi, F., Marmiroli, N., Maestri, E., 2018.
- 750 Structural and functional features of chars from different biomasses as potential plant amendments.
- 751 Front. Plant Sci. 9, 1119. https://doi.org/10.3389/FPLS.2018.01119/BIBTEX
- 752 Merino, D., Mansilla, A.Y., Casalongué, C.A., Alvarez, V.A., 2018. Preparation, characterization,
- and in vitro testing of nanoclay antimicrobial activities and elicitor capacity. J Agric Food Chem.
- 754 66(12), 3101-3109. https://doi.org/10.1021/acs.jafc.8b00049
- Mondani, L., Chiusa, G. Battilani, P., 2021. Chemical and biological control of Fusarium species
- 756 involved in garlic dry rot at early crop stages. Eur J Plant Pathol 160, 575-587.
- 757 <u>https://doi.org/10.1007/s10658-021-02265-0</u>
- Noman, M., Ahmed, T., Ijaz, U., Shahid, M., Nazir, M.M., Azizullah, White J.C., Li, D., Song F.,
- 759 2023. Bio-functionalized manganese nanoparticles suppress Fusarium wilt in watermelon
- 760 (Citrullus lanatus L.) by infection disruption, host defense response potentiation, and soil microbial
- 761 community modulation. Small. 19, e2205687. https://doi.org/10.1002/sml1.202205687
- Okungbowa, F.I., Shittu, H.O., 2012. Fusarium wilts: An overview. Environ. Res. J. 6, 83-102.
- Orr, R., Dennis, P.G., Wong, Y., Browne, D.J., Cooper, M., Birt, H.W.G., Lapis-Gaza, H.R.,
- Pattison, A.B., Nelson, P.N., 2022. Nitrogen fertilizer rate but not form affects the severity of
- 765 Fusarium wilt in banana. Front Plant Sci. 13, 907819. https://doi.org/10.3389/fpls.2022.907819
- Pavlicevic, M., Abdelraheem, W., Zuverza-Mena, N., O'Keefe, T., Mukhtar, S., Ridge, G.,
- Ranciato, J., Haynes, C., Elmer, W., Pignatello, J., Pagano, L., Caldara, M., Marmiroli, M.,
- Maestri, E., Marmiroli, N., White, J.C., 2022. Engineered nanoparticles, natural nanoclay and

- 769 biochar, as carriers of plant-growth promoting bacteria. Nanomaterials. 12(24), 4474.
- 770 <u>https://doi.org/10.3390/nano12244474</u>
- Plunkett, M.H., Knutson, C.M., Barney, B.M., 2020. Key factors affecting ammonium production
- by an *Azotobacter vinelandii* strain deregulated for biological nitrogen fixation. Microb. Cell Fact.
- 773 19, 107. https://doi.org/10.1186/s12934-020-01362-9
- Re, R., Pellegrini, N., Proteggente, A., Pannala, A., Yang, M., Rice-Evans, C., 1999. Antioxidant
- activity applying an improved ABTS radical cation decolorization assay. Free Radic. Biol. Med.
- 776 26, 1231-1237. https://doi.org/10.1016/S0891-5849(98)00315-3
- Saleh, A.E., Ul-Hassan, Z., Zeidan, R., Al-Shamary, N., Al-Yafei, T., Alnaimi, H., Higazy, N.S.,
- 778 Migheli, Q., Jaoua, S., 2021. Biocontrol activity of Bacillus megaterium BM344-1 against
- toxigenic fungi. ACS Omega. 6, 10984-10990. https://doi.org/10.1021/acsomega.1c00816
- 780 Sánchez-Moreno, C., Larrauri, J.A., Saura-Calixto, F., 1998. A procedure to measure the
- 781 antiradical efficiency of polyphenols. J. Sci. Food Agric. 76, 270-276.
- 782 https://doi.org/10.1002/(SICI)1097-0010(199802)76:2<270::AID-JSFA945>3.0.CO;2-9
- Seepe, H.A., Nxumalo, W., Amoo, S.O., 2021. Natural products from medicinal plants against
- 784 phytopathogenic Fusarium species: current research endeavours, challenges and prospects.
- 785 Molecules 26, 6539. https://doi.org/10.3390/molecules26216539
- Shah, I.H., Ashraf, M., Khan, A.R., Manzoor, M.A., Hayat, K., Arif, S., Sabir, I.A., Abdullah, M.,
- Niu, Q., Zhang, Y., 2022. Controllable synthesis and stabilization of Tamarix aphylla-mediated
- copper oxide nanoparticles for the management of Fusarium wilt on musk melon. 3 Biotech. 12,
- 789 128. https://doi.org/10.1007/s13205-022-03189-0

- 790 Shi, R-Y, Hong, Z-N., Li, J-J., Jiang, J., Abdulaha-Al Baquy, M. Xu, R-k., Qian, W., 2017.
- 791 Mechanisms for increasing the pH buffering capacity of an acidic ultisol by crop residue-derived
- 792 biochars. J. Agric. Food Chem. 65(37), 8111–8119. https://doi.org/10.1021/acs.jafc.7b02266
- Shoemaker, M., Cohen, I., Campbell, M., 2004. Reduction of MTT by aqueous herbal extracts in
- the absence of cells. J. Ethnopharmacol. 93, 381-384. https://doi.org/10.1016/j.jep.2004.04.011
- 795 Syed Nabi, R.B., Shahzad, R., Tayade, R., Shahid, M., Hussain, A., Ali, M.W., Yun, B.W., 2021.
- 796 Evaluation potential of PGPR to protect tomato against Fusarium wilt and promote plant growth.
- 797 PeerJ. 9, e11194. <u>https://doi.org/10.7717/peerj.11194</u>
- 798 Wahyuni, S., Wibowo, K.R.P., Prakoso, H.T., Bintang, M., Siswanto., 2021. Chitosan-Ag
- 799 nanoparticle antifungal activity against Fusarium sp., causal agent of wilt disease on chili. IOP
- 800 Conf. Ser.: Earth Environ. Sci. 948, 012064. https://doi.org/10.1088/1755-1315/948/1/012064
- Yan, Z., Chen, W.Q., van der Lee, T., Waalwijk, C., van Diepeningen, A.D., Feng, J., Zhang, H.,
- Liu, T.G., 2022. Evaluation of Fusarium head blight resistance in 410 Chinese wheat cultivars
- selected for their climate conditions and ecological niche using natural infection across three
- distinct experimental sites. Front. Plant Sci. 13, 916282. https://doi.org/10.3389/fpls.2022.916282
- 805 Yuan, Q-S., Wang, L., Wang, H., Wang, X., Jiang, W., Ou, X., Xiao, C., Gao, Y., Xu, J., Yang,
- 806 Y., Cui, X., Guo, L., Huang, L., Zhou, T., 2022. Pathogen-mediated assembly of plant-beneficial
- bacteria to alleviate Fusarium wilt in *Pseudostellaria heterophylla*. Front. Microbiol. 13, 842372.
- 808 https://doi.org/10.3389/fmicb.2022.842372
- 809 Zhang, K., Wang, L., Si, H., Guo, H., Liu, J., Jia, J., Su, Q., Wang, Y., Zang, J., Xing, J., Dong, J.,
- 810 2022. Maize stalk rot caused by Fusarium graminearum alters soil microbial composition and is
- directly inhibited by Bacillus siamensis isolated from rhizosphere soil. Front. Microbiol. 13,
- 986401. https://doi.org/10.3389/fmicb.2022.986401

813	Zhang, Y., He, J., Jia, L.J., Yuan, T.L., Zhang, D., Guo, Y., Wang, Y., Tang, W.H., 2016. Cellular
814	tracking and gene profiling of Fusarium graminearum during maize stalk rot disease development
815	elucidates its strategies in confronting phosphorus limitation in the host apoplast. PLoS Pathog.
816	12, e1005485. https://doi.org/10.1371/journal.ppat.1005485
817	Zhou, X., Wang, J., Liu, F., Liang, J., Zhao, P., Tsui, C.K.M., Cai, L., 2022. Cross-kingdom
818	synthetic microbiota supports tomato suppression of Fusarium wilt disease. Nat. Commun. 13,
819	7890. https://doi.org/10.1038/s41467-022-35452-6
820	Zibanezhadian, M., Sardrood, B.P., Taheri, H., Farkhari, M., 2020. Anti-oxidative response of
821	Bacillus thuringiensis-primed tomato plants to Fusarium oxysporum f. sp. Lycopersici. J. Plant
822	Mol. Breed. 8(2), 29 – 37. https://doi.org/10.22058/JPMB.2022.543818.1245

Figure Captions

Figure 1: Total chlorophylls content. A- tomato; B- watermelon. Abbreviations: C – control plants; F- Fusarium infected plants; B+ F – Fusarium infected plants with bacteria added to the soil; MSN +F – Fusarium infected plants treated with chitosan-coated mesoporous silica nanoparticles; NC + F – Fusarium infected plants treated with nanoclay; IB + F – Fusarium infected plants treated with "Italian" biochar; AB+F – Fusarium infected plants treated with Aries Green biochar; NB + F – Fusarium infected plants treated with Naked biochar; MSN + B + F – Fusarium infected plants treated with chitosan-coated mesoporous silica nanoparticles with adsorbed bacteria; NC + B +F – Fusarium infected plants treated with "Italian" biochar with adsorbed bacteria; AB +B +F – Fusarium infected plants treated with Aries Green biochar with adsorbed bacteria; NB +B +F – Fusarium infected plants treated with Naked biochar with adsorbed bacteria; NB +B +F – Fusarium infected plants treated with Naked biochar with adsorbed bacteria; NB +B +F – Fusarium infected plants treated with Naked biochar with adsorbed bacteria; NB +B +F – Fusarium infected plants treated with Naked biochar with adsorbed bacteria.

836	Different letters for the same time point means that differences between samples were statistically
837	significant (determined by Tukey test at $p < 0.05$)
838	Figure 2: Viability. A- tomato; B- watermelon. Abbreviations: C – control plants; F- Fusarium
839	infected plants; B+ F $-$ Fusarium infected plants with bacteria added to the soil; MSN +F $-$
840	Fusarium infected plants treated with chitosan-coated mesoporous silica nanoparticles; $NC + F -$
841	Fusarium infected plants treated with nanoclay; IB + F - Fusarium infected plants treated with
842	"Italian" biochar; AB+ F – Fusarium infected plants treated with Aries Green biochar; NB + F –
843	Fusarium infected plants treated with Naked biochar; MSN + B + F- Fusarium infected plants
844	treated with chitosan-coated mesoporous silica nanoparticles with adsorbed bacteria; $NC + B + F$
845	- Fusarium infected plants treated with nanoclay with adsorbed bacteria; IB +B + F- Fusarium
846	infected plants treated with "Italian" biochar with adsorbed bacteria; AB +B +F - Fusarium
847	infected plants treated with Aries Green biochar with adsorbed bacteria; NB +B +F - Fusarium
848	infected plants treated with Naked biochar with adsorbed bacteria. Different letters for the same
849	time point means that differences between samples were statistically significant (determined by
850	Tukey test at $p < 0.05$)
851	Figure 3: Representation of different treatments. A-left: Fusarium infected control plant (F); right:
852	Fusarium infected plant treated with bacteria added directly into soil (B+F); B- right: Fusarium
853	infected plant treated with chitosan-coated mesoporous silica nanoparticles (MSN+F); left:
854	Fusarium infected plant treated with chitosan-coated mesoporous silica with adsorbed bacteria
855	(MSN+F+B); C- right: Fusarium infected plant treated with nanoclay with adsorbed bacteria
856	(NC+F+B); left: Fusarium infected plant treated with nanoclay (NC+F); D- right: Fusarium
857	infected plant treated with "Italian" biochar (IB+F); left: Fusarium infected plant treated with
858	"Italian" biochar with adsorbed bacteria (IB+F+B); E- right: Fusarium infected plant treated with

Aries biochar with adsorbed bacteria (AB+F+B); left: Fusarium infected plant treated with Aries 859 biochar (AB+F); F- right: Fusarium infected plant treated with Naked biochar (NB+F); left: 860 Fusarium infected plant treated with Naked biochar with adsorbed bacteria (NB+F+B); G-left: 861 control, healthy plant (C); right-Fusarium infected control plant (F). 862 Figure 4: Content of antioxidants determined by DPPH test. A- tomato; B- watermelon. 863 864 Abbreviations: C – control plants; F- Fusarium infected plants; B+ F – Fusarium infected plants with bacteria added to the soil; MSN +F – Fusarium infected plants treated with chitosan-coated 865 mesoporous silica nanoparticles; NC + F – Fusarium infected plants treated with nanoclay; IB + F 866 - Fusarium infected plants treated with "Italian" biochar; AB+ F - Fusarium infected plants treated 867 with Aries Green biochar; NB + F - Fusarium infected plants treated with Naked biochar; MSN 868 + B + F- Fusarium infected plants treated with chitosan-coated mesoporous silica nanoparticles 869 with adsorbed bacteria; NC + B +F – Fusarium infected plants treated with nanoclay with adsorbed 870 bacteria; IB +B + F- Fusarium infected plants treated with "Italian" biochar with adsorbed 871 bacteria; AB +B +F – Fusarium infected plants treated with Aries Green biochar with adsorbed 872 bacteria; NB +B +F – Fusarium infected plants treated with Naked biochar with adsorbed bacteria. 873 Different letters for the same time point means that differences between samples were statistically 874 875 significant (determined by Tukey test at p < 0.05) Figure 5: Content of total bacteria. A- tomato; B- watermelon. Abbreviations: C – control plants; 876 877 F- Fusarium infected plants; B+ F – Fusarium infected plants with bacteria added to the soil; MSN 878 +F – Fusarium infected plants treated with chitosan-coated mesoporous silica nanoparticles; NC + F – Fusarium infected plants treated with nanoclay; IB + F – Fusarium infected plants treated with 879 "Italian" biochar; AB+ F – Fusarium infected plants treated with Aries Green biochar; NB + F – 880 881 Fusarium infected plants treated with Naked biochar; MSN + B + F- Fusarium infected plants

treated with chitosan-coated mesoporous silica nanoparticles with adsorbed bacteria; NC + B +F 882 - Fusarium infected plants treated with nanoclay with adsorbed bacteria; IB +B + F- Fusarium 883 infected plants treated with "Italian" biochar with adsorbed bacteria; AB +B +F - Fusarium 884 infected plants treated with Aries Green biochar with adsorbed bacteria; NB +B +F - Fusarium 885 infected plants treated with Naked biochar with adsorbed bacteria. Different letters for the same 886 887 time point means that differences between samples were statistically significant (determined by Tukey test at p < 0.05) 888 Figure 6: Content of N-fixing bacteria. A- tomato; B- watermelon. Abbreviations: C – control 889 plants; F- Fusarium infected plants; B+ F - Fusarium infected plants with bacteria added to the 890 soil; MSN +F - Fusarium infected plants treated with chitosan-coated mesoporous silica 891 nanoparticles; NC + F - Fusarium infected plants treated with nanoclay; IB + F - Fusarium 892 infected plants treated with "Italian" biochar; AB+ F – Fusarium infected plants treated with Aries 893 Green biochar; NB + F - Fusarium infected plants treated with Naked biochar; MSN + B + F-894 Fusarium infected plants treated with chitosan-coated mesoporous silica nanoparticles with 895 adsorbed bacteria; NC + B +F - Fusarium infected plants treated with nanoclay with adsorbed 896 bacteria; IB +B + F- Fusarium infected plants treated with "Italian" biochar with adsorbed 897 898 bacteria; AB +B +F - Fusarium infected plants treated with Aries Green biochar with adsorbed bacteria; NB +B +F – Fusarium infected plants treated with Naked biochar with adsorbed bacteria. 899 900 Different letters for the same time point means that differences between samples were statistically 901 significant (determined by Tukey test at p < 0.05) Figure 7: Content of P-solubilizing bacteria. A- tomato; B- watermelon. Abbreviations: C – 902 903 control plants; F- Fusarium infected plants; B+ F - Fusarium infected plants with bacteria added 904 to the soil; MSN +F - Fusarium infected plants treated with chitosan-coated mesoporous silica

nanoparticles; NC + F - Fusarium infected plants treated with nanoclay; IB + F - Fusarium
infected plants treated with "Italian" biochar; AB+ F - Fusarium infected plants treated with Aries
Green biochar; NB + F - Fusarium infected plants treated with Naked biochar; MSN + B + F-
Fusarium infected plants treated with chitosan-coated mesoporous silica nanoparticles with
adsorbed bacteria; NC + B +F - Fusarium infected plants treated with nanoclay with adsorbed
bacteria; IB +B + F- Fusarium infected plants treated with "Italian" biochar with adsorbed
bacteria; AB +B +F - Fusarium infected plants treated with Aries Green biochar with adsorbed
bacteria; NB +B +F – Fusarium infected plants treated with Naked biochar with adsorbed bacteria
Different letters for the same time point means that differences between samples were statistically
significant (determined by Tukey test at p < 0.05)

<u>Tables</u>

 Table 1. Treatments used in experiments

	control (C)				
	Plants infected with Fusarium (F)				
	Plants infected with Fusarium with added bacteria (B + F)				
chitosan-coated mesoporous silica (MSN)	infected plants treated with chitosan-coated mesoporous silica (MSN+F)	infected plants treated with chitosan- coated mesoporous silica with loaded bacteria (MSN+B+F)			
Nanoclay (NC)	infected plants treated with nanoclay (NC+F)	infected plants treated with nanoclay with loaded bacteria (NC+B+F)			
"Italian" biochar (IB)	infected plants treated with "Italian" biochar (IB+F)	infected plants treated with "Italian" biochar with loaded bacteria (IB+B+F)			
Aries biochar (AB)	infected plants treated Aries green biochar (AB+F)	infected plants treated with Aries Green biochar with loaded bacteria (AB+B+F)			
Naked biochar (NB)	infected plants treated with Naked biochar (NB+F)	infected plants treated with Naked biochar with loaded bacteria (NB+B+F)			

Table 2: Nitrogen content in Fusarium-infected plants in tomato and watermelon experiments*

	N content (mg/g)							
		Tomato e	xperiment			Watermelo	n experiment	
samples	0 days	7 days	14 days	28 days	0 days	10 days	20 days	30 days
С	57.1±1.2 ^a	54.8±2.0 ^{a,b}	41.4±2.8ª	23.1±2.2ª	29.9±3.1ª	25.4±1.4 ^a	18.5±1.3 ^a	17.7±1.5 ^a
F	57.1±1.2 ^a	42.2±3.9°	35.2±3.3ª	51.4±2.9 ^{b,c}	29.9±3.1ª	41.3±4.0 ^b	44.8±1.5 ^b	50.7±4.8 ^b
B + F	57.1±1.2 ^a	$47.3 \pm 1.9^{a,b,d}$	39.4±2.8ª	49.5±3.0 ^{b,c,d}	29.9±3.1ª	47.2±4.9 ^b	47.7±5.4 ^{b,c}	51.0±5.3 ^b
MSN + F	57.1±1.2 ^a	42.5±3.0°	35.4±2.2ª	61.6±3.4°	29.9±3.1ª	45.5±1.5 ^b	34.6±2.9 ^d	22.7±2.2 ^{a,c}
NC + F	57.1±1.2 ^a	49.1±3.1 ^{a,b,d}	36.9±4.0ª	41.7±3.3 ^{f,g}	29.9±3.1ª	41.9±1.2 ^b	54.6±2.9°	33.8±3.5 ^d
IB+F	57.1±1.2 ^a	42.4±3.6°	36.3±3.3ª	56.9±3.8 ^{b,c,h}	29.9±3.1ª	36.9±4.7 ^{a,b}	44.9±1.7 ^b	44.8±3.6°
AB + F	57.1±1.2 ^a	46.2±2.5 ^{a,c,d}	33.2±3.8ª	34.0±2.9i	29.9±3.1ª	46.4±5.1 ^b	35.6±1.8 ^d	47.1±2.9 ^{b,f}
NB + F	57.1±1.2 ^a	49.6±4.4 ^{a,c,d}	34.1±3.9 ^a	44.5±4.0 ^{f,g, j}	29.9±3.1ª	47.9±4.8 ^b	47.4±2.4 ^{b,c}	50.8±3.1 ^b
MSN + B +F	57.1±1.2 ^a	45.2±1.5 ^{c,d}	34.2±3.5 ^a	40.7±3.8 ^f	29.9±3.1ª	35.1±4.3 ^{a,b}	50.3±1.3 ^{b,c}	52.0±4.7 ^{b,g}
NC + B + F	57.1±1.2 ^a	58.0±4.7 ^b	36.5±1.9 ^a	52.5±4.1°	29.9±3.1ª	43.0±5.1 ^b	46.9±1.4 ^b	38.4±2.4 ^{d,h}
IB+B+F	57.1±1.2 ^a	51.3±5.0 ^{a,b,d}	35.7±3.9 ^a	52.9±4.4°	29.9±3.1ª	41.3±2.2 ^b	44.5±1.8 ^b	47.4±4.0 ^{b,f}
AB+B+F	57.1±1.2 ^a	48.1±2.8 ^{a,c,d}	35.8±2.2ª	47.6±3.6 ^k	29.9±3.1ª	44.2±2.4 ^b	43.6±1.2 ^b	48.3±3.6 ^{b,f}
NB + B + F	57.1±1.2 ^a	53.5±1.6 ^{a,b,d}	33.9±3.3ª	48.1±2.9 ^{b,k}	29.9±3.1ª	37.8±4.5 ^{a,b}	47.4±2.3 ^{b,c}	45.2±2.9 ^e

^{*} Different letters at the same column means that differences between samples were statistically significant (determined by Tukey test). Abbreviations: C – control plants; F- Fusarium infected plants; B + F – Fusarium infected plants with bacteria added to the soil; MSN + F – Fusarium infected plants treated with chitosan-coated mesoporous silica nanoparticles; NC + F – Fusarium infected plants treated with nanoclay; IB + F – Fusarium infected plants treated with "Italian" biochar; AB + F – Fusarium infected plants treated with Naked biochar; MSN + B + F – Fusarium infected plants treated with chitosan-coated mesoporous silica nanoparticles with adsorbed bacteria; NC + B + F – Fusarium infected plants treated with nanoclay with adsorbed bacteria; IB + B + F – Fusarium infected plants treated with "Italian" biochar with adsorbed bacteria; AB + B + F – Fusarium infected plants treated with Aries Green biochar with adsorbed bacteria; NB + B + F – Fusarium infected plants treated with Naked biochar with adsorbed bacteria.

Table 3: Phosphorus content in *Fusarium*-infected plants in tomato and watermelon experiments*

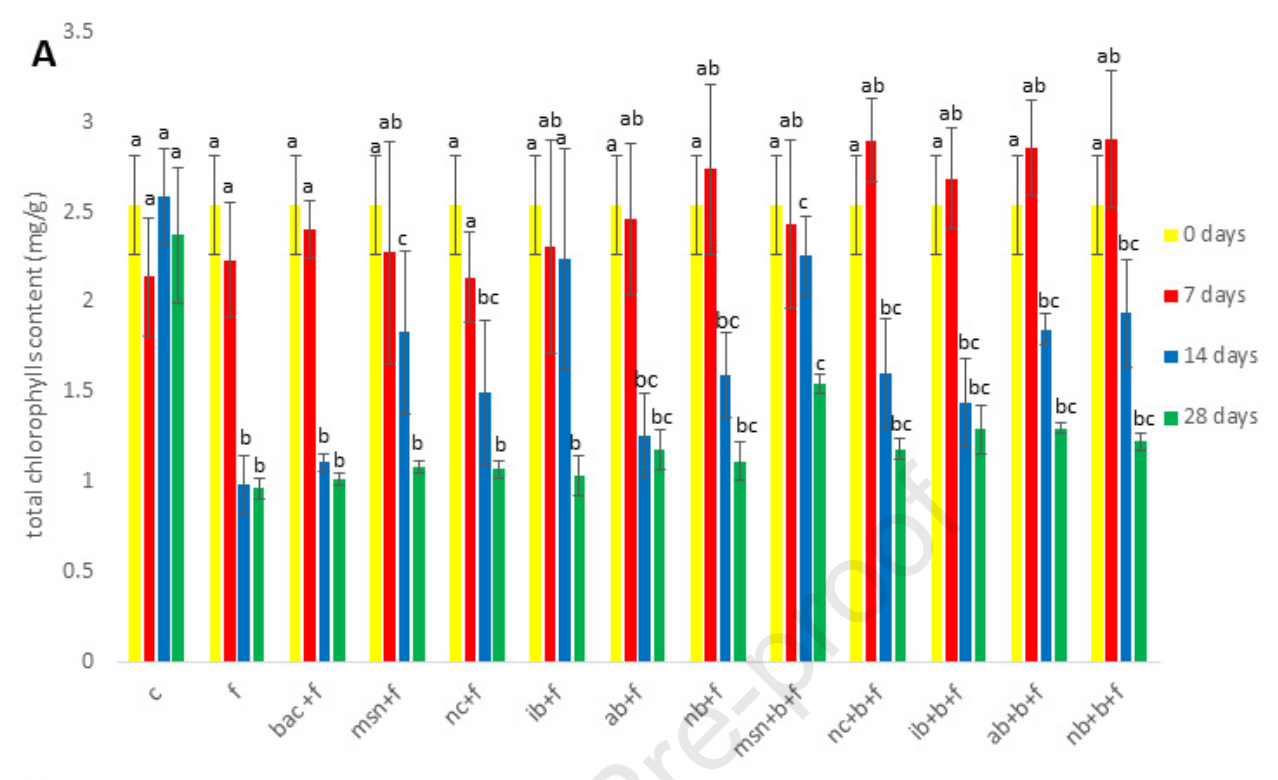
	P content (mg/g)							
		Tomato	experiment			Watermelo	n experimen	t
samples	0 days	7 days	14 days	28 days	0 days	10 days	20 days	30 days
С	9.3±0.5 ^a	7.2±1.0 ^a	7.0±1.3 ^b	3.0±0.4 ^a	4.3±0.8 ^a	4.7±0.6 ^a	1.9±0.3ª	1.7±0.2ª
F	9.3±0.5ª	6.1±0.4 ^b	6.8±1.0 ^b	10.0±0.3 ^{b,c}	4.3±0.8 ^a	3.2±0.4 ^b	5.9±0.1 ^b	6.2±0.2 ^b
B+F	9.3±0.5 ^a	4.0±0.2 ^{c,d}	8.0±0.4 ^b	12.7±0.1 ^d	4.3±0.8 ^a	5.1±0.6 ^e	5.4±0.8°	6.1±0.1 ^b
MSN + F	9.3±0.5 ^a	3.5±0.3 ^d	7.6±0.2b	11.7±0.1e	4.3±0.8 ^a	4.2±0.4 ^{a,d}	3.8±0.6 ^d	5.3±0.1 ^d
NC + F	9.3±0.5ª	2.6±0.5 ^d	8.0±0.7 ^b	11.0±0.2 ^f	4.3±0.8 ^a	4.6±0.5 ^{a,e}	6.3±0.2 ^{b,e}	5.2±0.7 ^{d,e}
IB+F	9.3±0.5 ^a	3.1±0.5 ^d	6.4±0.5 ^{b,c}	10.1±0.2 ^{b,c}	4.3±0.8 ^a	3.8±0.5 ^{c,d}	5.3±0.1°	5.3±0.8 ^e
AB + F	9.3±0.5 ^a	3.3±0.6 ^d	7.4±0.3 ^b	10.2±0.3°	4.3±0.8 ^a	6.2±0.8 ^f	5.8±0.8 ^b	4.1±0.6 ^f
NB + F	9.3±0.5 ^a	3.6±0.7 ^{c,d}	7.0±0.6 ^b	9.8±0.3 ^b	4.3±0.8 ^a	6.3±0.7 ^f	7.0±1.0 ^f	5.0±0.8g
MSN + B +F	9.3±0.5 ^a	5.9±0.6 ^{b,c}	6.4±1.0 ^{b,c}	10.0±0.1 ^{b,c}	4.3±0.8 ^a	3.7±0.4 ^{c,d}	4.6±0.6 ^g	6.2±0.9 ^{b,h}
NC + B + F	9.3±0.5 ^a	3.2±0.5 ^d	5.2±0.9 ^{a,c}	11.7±0.2 ^e	4.3±0.8 ^a	4.7±0.4 ^{a,e}	4.8±0.1 ^{g,h}	5.8±0.8 ⁱ
IB + B + F	9.3±0.5 ^a	2.0±0.3 ^e	4.9±0.4 ^a	11.9±0.1e	4.3±0.8 ^a	3.6±0.6°	5.2±0.2 ^{c,i}	6.3±0.9 ^h
AB + B +F	9.3±0.5 ^a	2.5±0.5 ^{e,d}	5.8±0.3°	9.8±0.2 ^b	4.3±0.8 ^a	3.4±0.5 ^{b,c}	6.0±0.7 ^b	6.7±1 ^j
NB + B + F	9.3±0.5 ^a	2.4±0.4 ^e	6.7±0.7 ^b	11.0±0.3 ^f	4.3±0.8 ^a	3.5±0.4 ^{b,c}	4.9±0.1 ^{g,h}	6.2±0.8 ^{b,c}

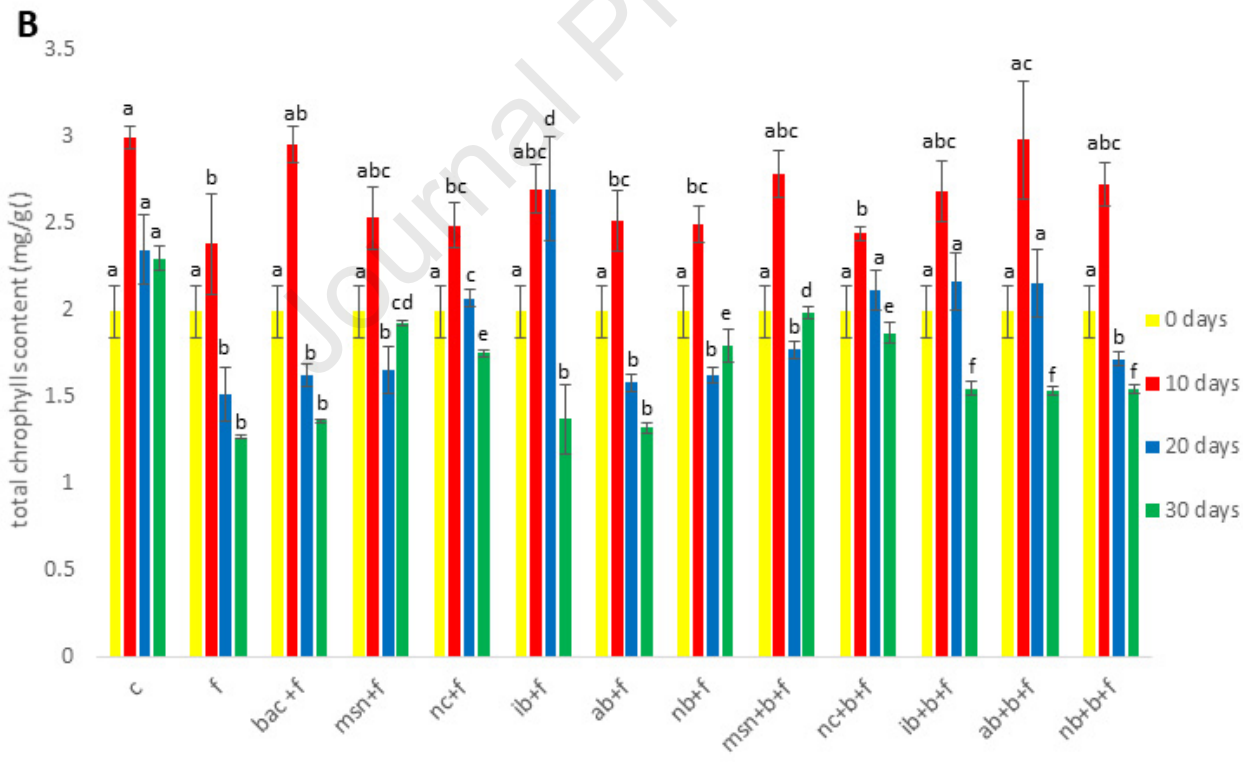
^{*} Different letters at the same column means that differences between samples were statistically significant (determined by Tukey test). Abbreviations: C – control plants; F- Fusarium infected plants; B + F – Fusarium infected plants with bacteria added to the soil; MSN +F – Fusarium infected plants treated with chitosan-coated mesoporous silica nanoparticles; NC + F – Fusarium infected plants treated with nanoclay; IB + F – Fusarium infected plants treated with "Italian" biochar; AB+ F – Fusarium infected plants treated with Aries Green biochar; NB + F – Fusarium infected plants treated with Naked biochar; MSN + B + F – Fusarium infected plants treated with nanoclay with adsorbed bacteria; IB +B + F – Fusarium infected plants treated with "Italian" biochar with adsorbed bacteria; AB +B +F – Fusarium infected plants treated with Aries Green biochar with adsorbed bacteria; NB +B +F – Fusarium infected plants treated with Aries Green biochar with adsorbed bacteria; NB +B +F – Fusarium infected plants treated with Naked biochar with adsorbed bacteria.

Table 4: Soil pH in Fusarium-infected plants in tomato and watermelon experiments*

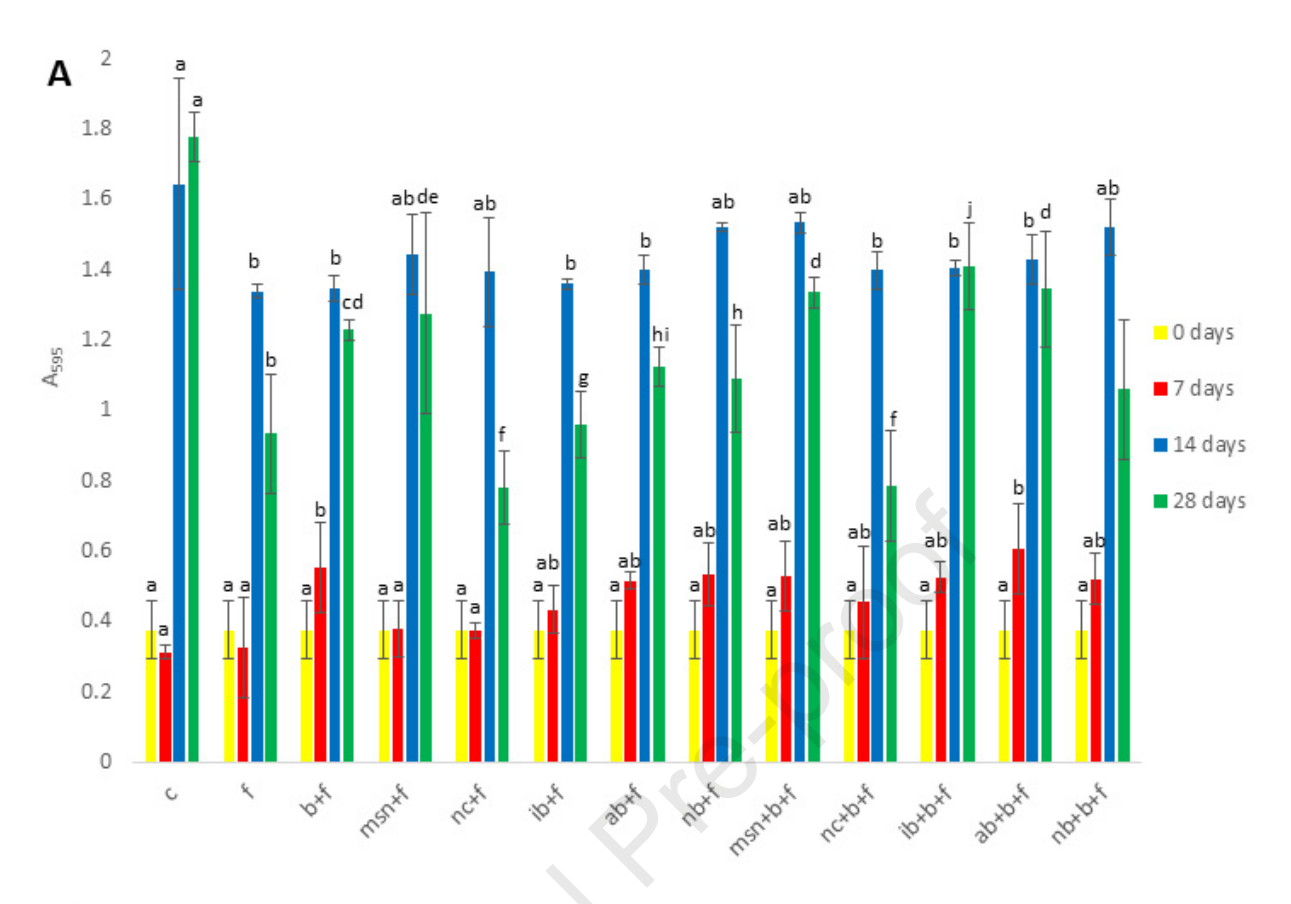
	рН							
		Tomato	experiment			Watermelo	n experiment	
samples	0 days	7 days	14 days	28 days	0 days	10 days	20 days	30 days
С	5.66±0.08 ^a	5.82±0.04 ^a	6.05±0.08 ^a	6.16±0.12 ^a	5.66±0.08°	6.18±0.10 ^a	6.28±0.12 ^{a,b}	6.36±0.13 ^a
F	5.66±0.08°	5.96±0.10 ^a	6.19±0.10 ^{a,b}	5.98±0.11 ^a	5.66±0.08 ^a	6.56±0.10 ^b	6.24±0.13 ^{a,b}	6.42±0.03 ^a
B + F	5.66±0.08 ^a	5.93±0.02ª	6.26±0.11 ^{a,b}	5.86±0.11 ^a	5.66±0.08 ^a	6.94±0.11°	6.44±0.12 ^{a,b}	6.41±0.11 ^a
MSN + F	5.66±0.08 ^a	6.02±0.10 ^a	6.14±0.08 ^{a,b}	6.01±0.12 ^a	5.66±0.08°	6.67±0.12 ^b	6.39±0.13 ^{a,b}	6.62±0.05 ^b
NC + F	5.66±0.08 ^a	6.00±0.11 ^a	6.33±0.13 ^b	6.04±0.07 ^a	5.66±0.08 ^a	6.82±0.07°	6.43±0.10 ^a	6.30±0.11 ^a
IB+F	5.66±0.08 ^a	5.94±0.03 ^a	6.18±0.09 ^{a,b}	6.05±0.12 ^a	5.66±0.08 ^a	6.93±0.14°	6.22±0.03 ^{a,b}	6.36±0.12 ^a
AB + F	5.66±0.08 ^a	5.95±0.02 ^a	6.14±0.04 ^{a,b}	6.09±0.08 ^a	5.66±0.08 ^a	6.54±0.13 ^b	6.38±0.10 ^{a,b}	6.35±0.13 ^a
NB + F	5.66±0.08 ^a	6.01±0.04 ^a	6.08±0.09 ^{a,b}	6.03±0.12 ^a	5.66±0.08 ^a	6.39±0.12 ^{a,b}	6.02±0.11 ^b	6.27±0.11 ^a
MSN + B +F	5.66±0.08 ^a	6.00±0.11 ^a	6.18±0.06 ^{ab}	5.99±0.09 ^a	5.66±0.08 ^a	6.34±0.10 ^{a,b}	6.15±0.07 ^{a,b}	6.24±0.10 ^a
NC + B + F	5.66±0.08 ^a	5.80±0.10 ^a	6.22±0.12 ^{a,b}	6.01±0.04 ^a	5.66±0.08 ^a	6.38±0.11 ^{a,b}	6.28±0.08 ^{a,b}	6.28±0.07 ^a
IB + B + F	5.66±0.08 ^a	6.10±0.06 ^a	6.16±0.06 ^{a,b}	5.97±0.09 ^a	5.66±0.08 ^a	6.57±0.13 ^b	6.23±0.05 ^{a,b}	6.25±0.13 ^a
AB + B +F	5.66±0.08 ^a	5.97±0.09 ^a	6.17±0.02 ^{a,b}	6.08±0.07 ^a	5.66±0.08 ^a	6.66±0.12 ^b	6.22±0.13 ^{a,b}	6.19±0.09 ^a
NB + B + F	5.66±0.08 ^a	6.05±0.09 ^a	6.14±0.11 ^{a,b}	6.16±0.11 ^a	5.66±0.08 ^a	6.68±0.13 ^b	6.26±0.12 ^{a,b}	6.24±0.12 ^a

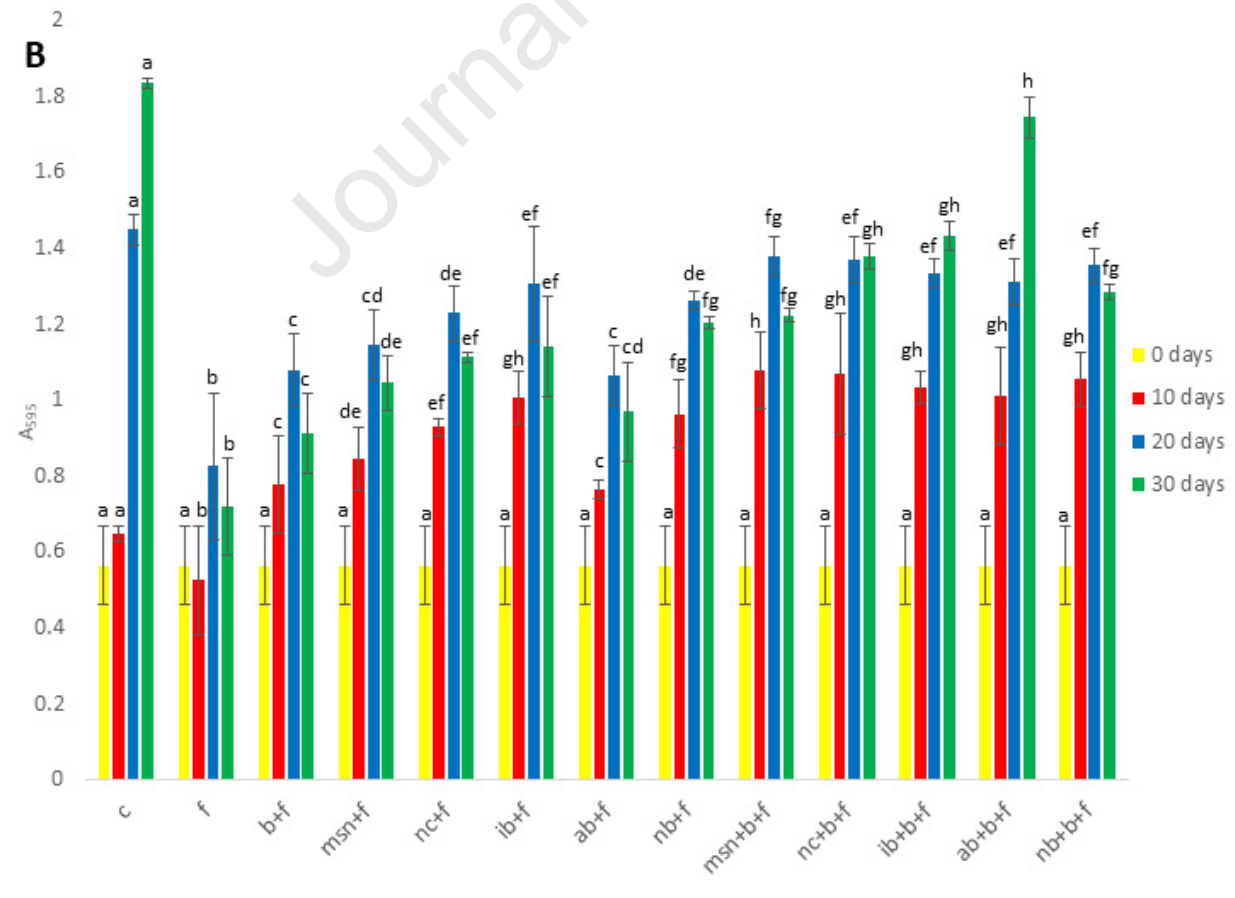
^{*} Different letters at the same column means that differences between samples were statistically significant (determined by Tukey test). Abbreviations: C – control plants; F- Fusarium infected plants; B + F – Fusarium infected plants with bacteria added to the soil; MSN +F – Fusarium infected plants treated with chitosan-coated mesoporous silica nanoparticles; NC + F – Fusarium infected plants treated with nanoclay; IB + F – Fusarium infected plants treated with "Italian" biochar; AB+ F – Fusarium infected plants treated with Naked biochar; MSN + B + F – Fusarium infected plants treated with chitosan-coated mesoporous silica nanoparticles with adsorbed bacteria; NC + B +F – Fusarium infected plants treated with nanoclay with adsorbed bacteria; IB +B + F – Fusarium infected plants treated with "Italian" biochar with adsorbed bacteria; AB +B +F – Fusarium infected plants treated with Aries Green biochar with adsorbed bacteria; NB +B +F – Fusarium infected plants treated with Naked biochar with adsorbed bacteria.





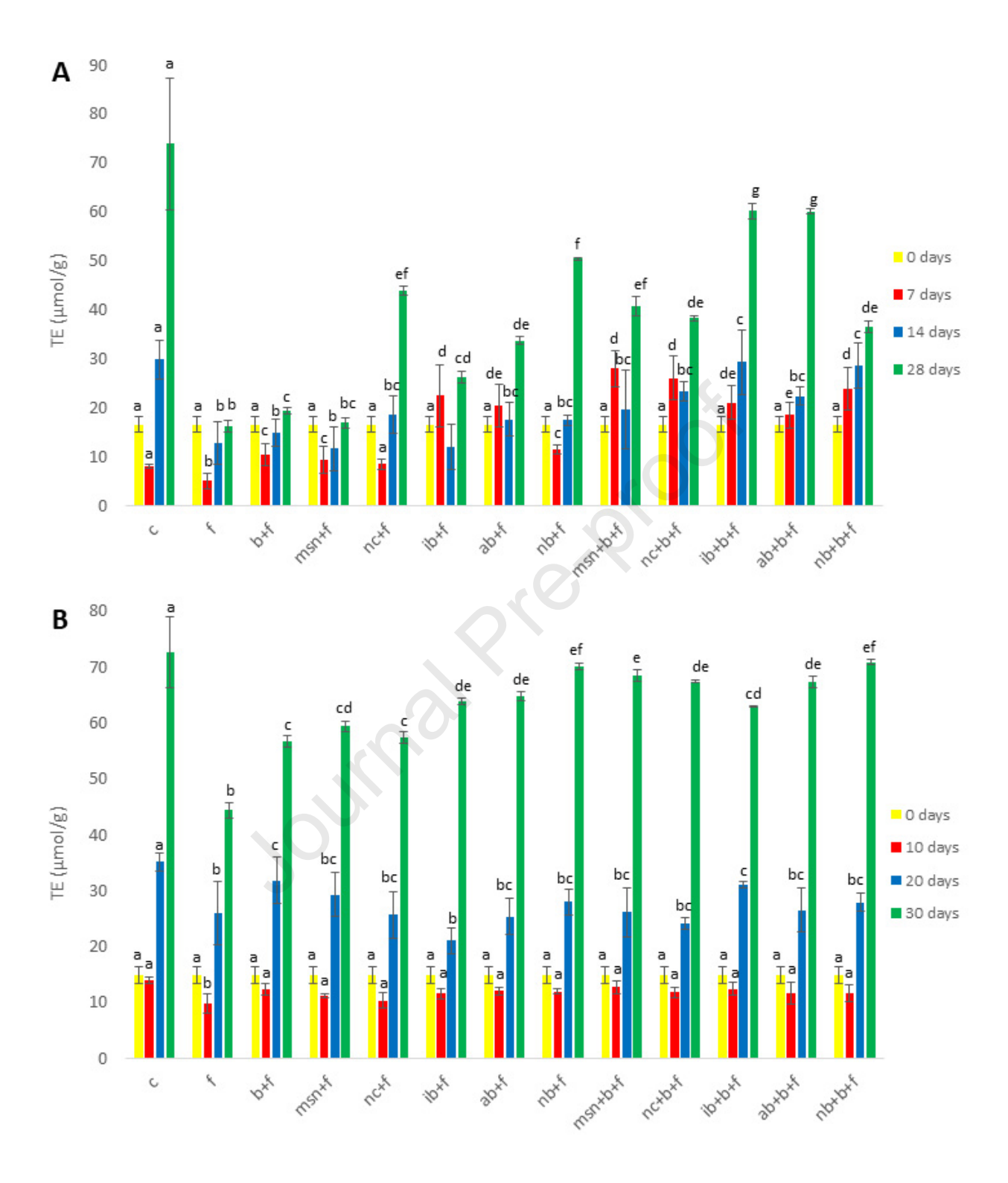
John Richard Control

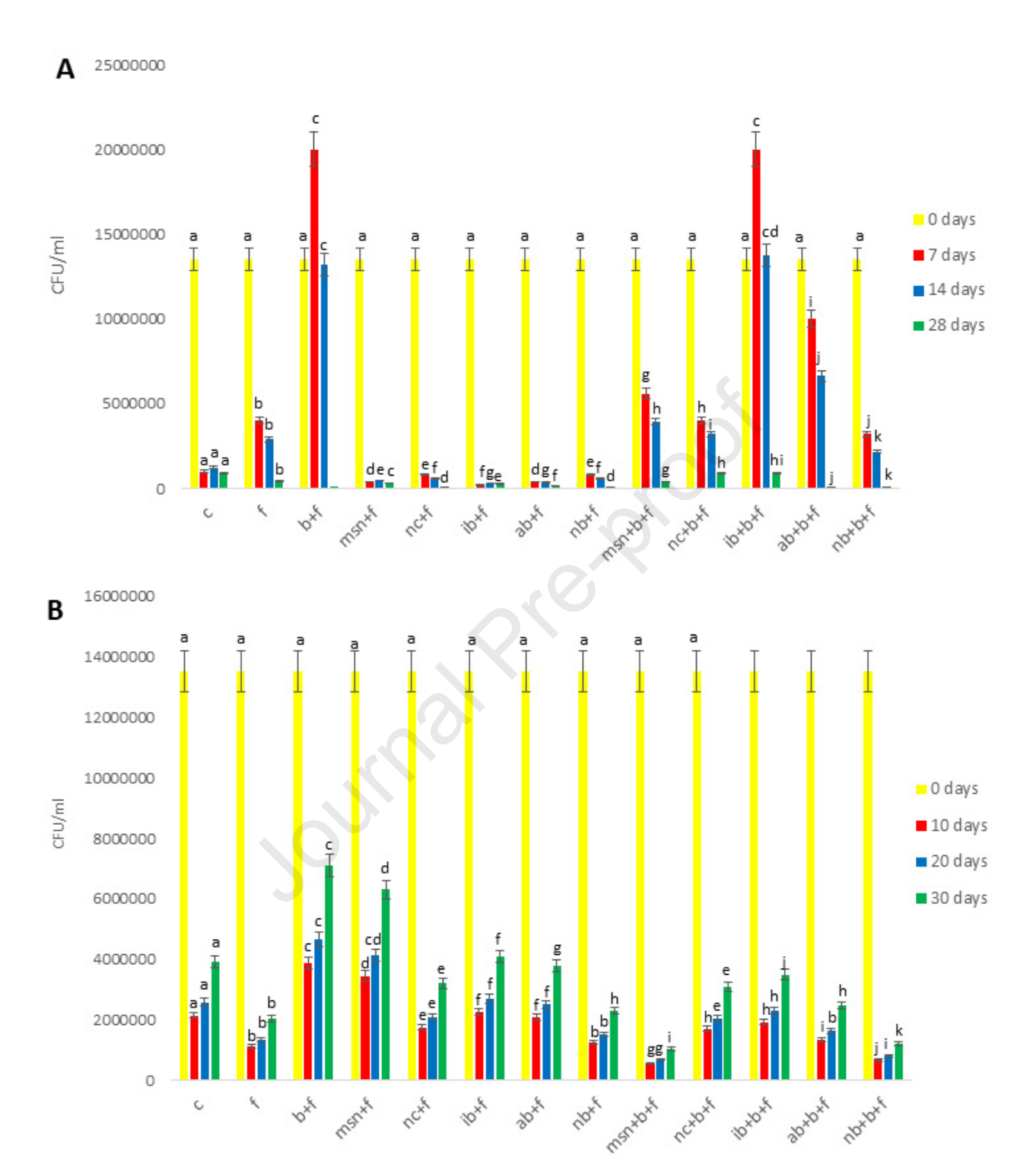


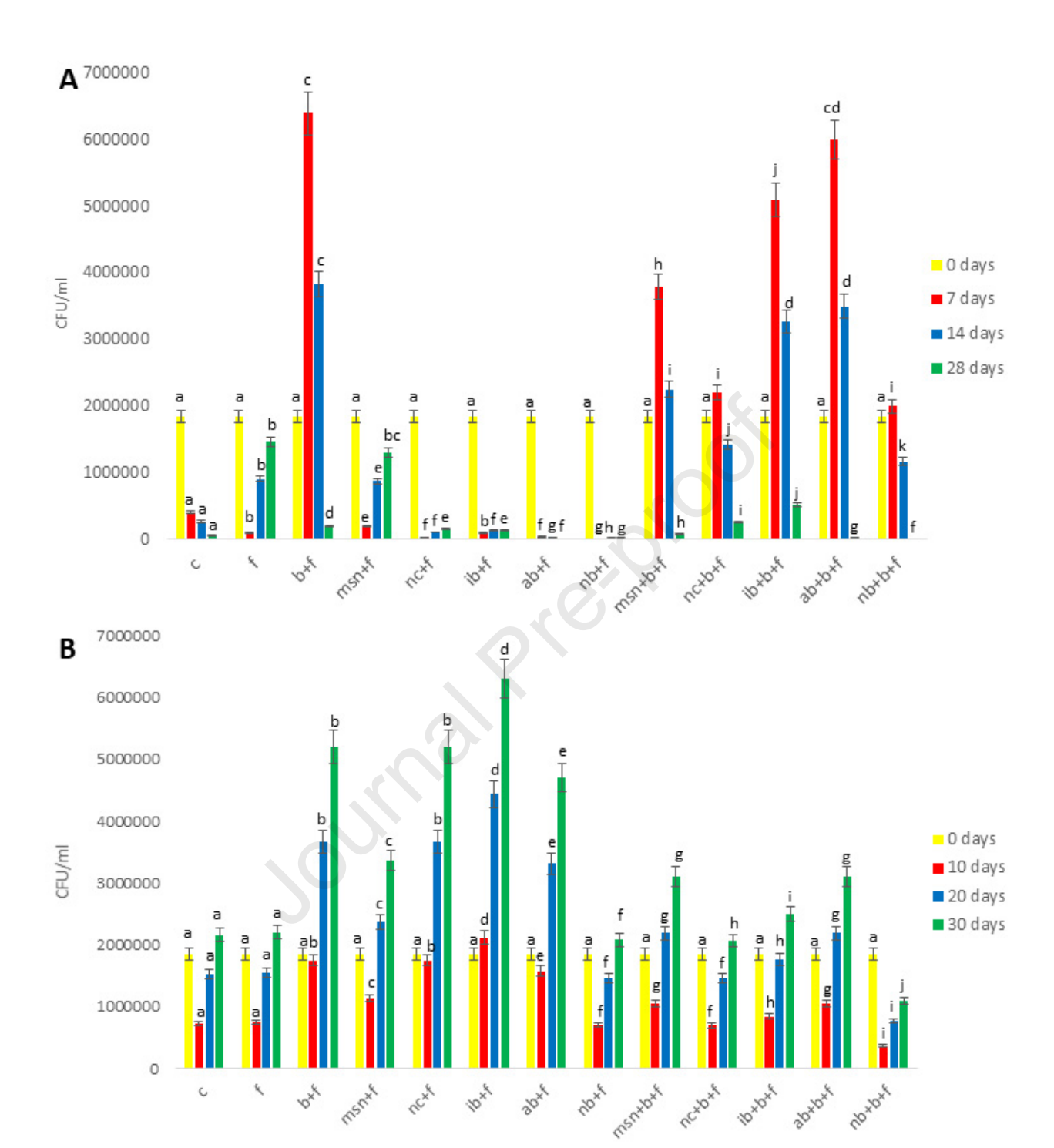


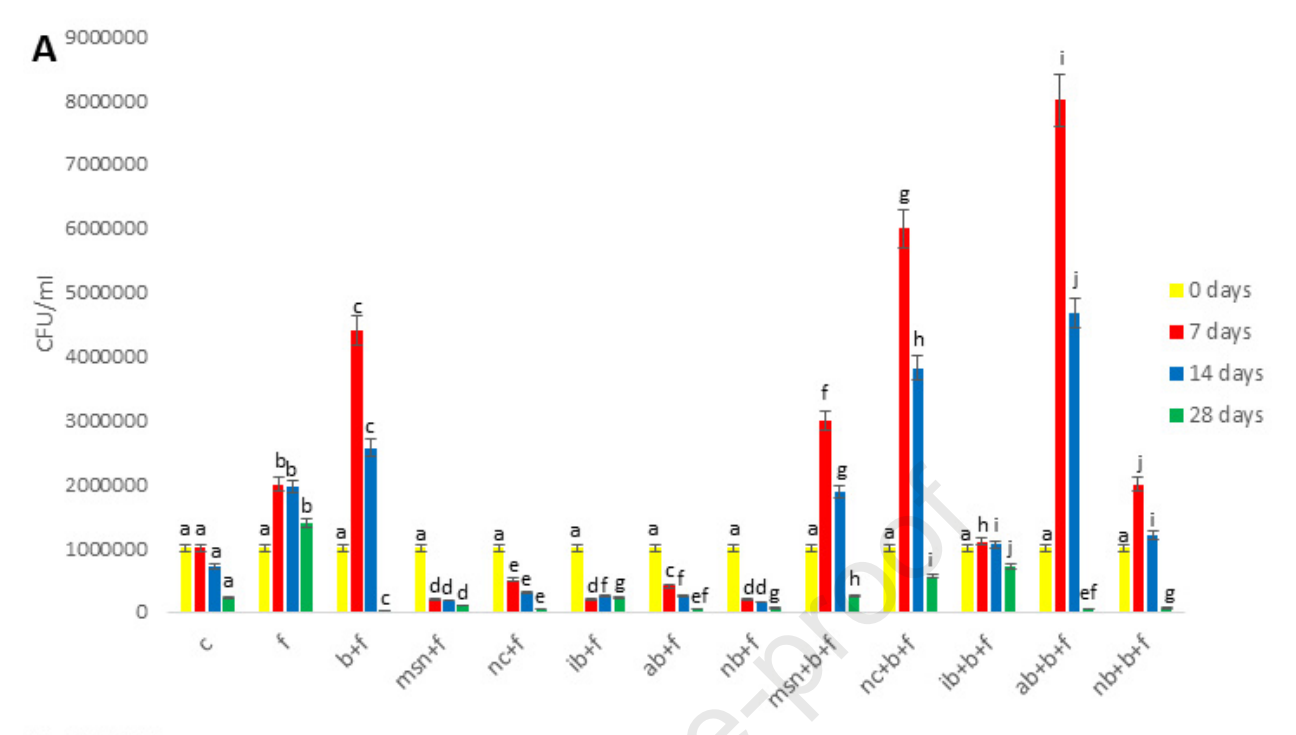
John Richard Control

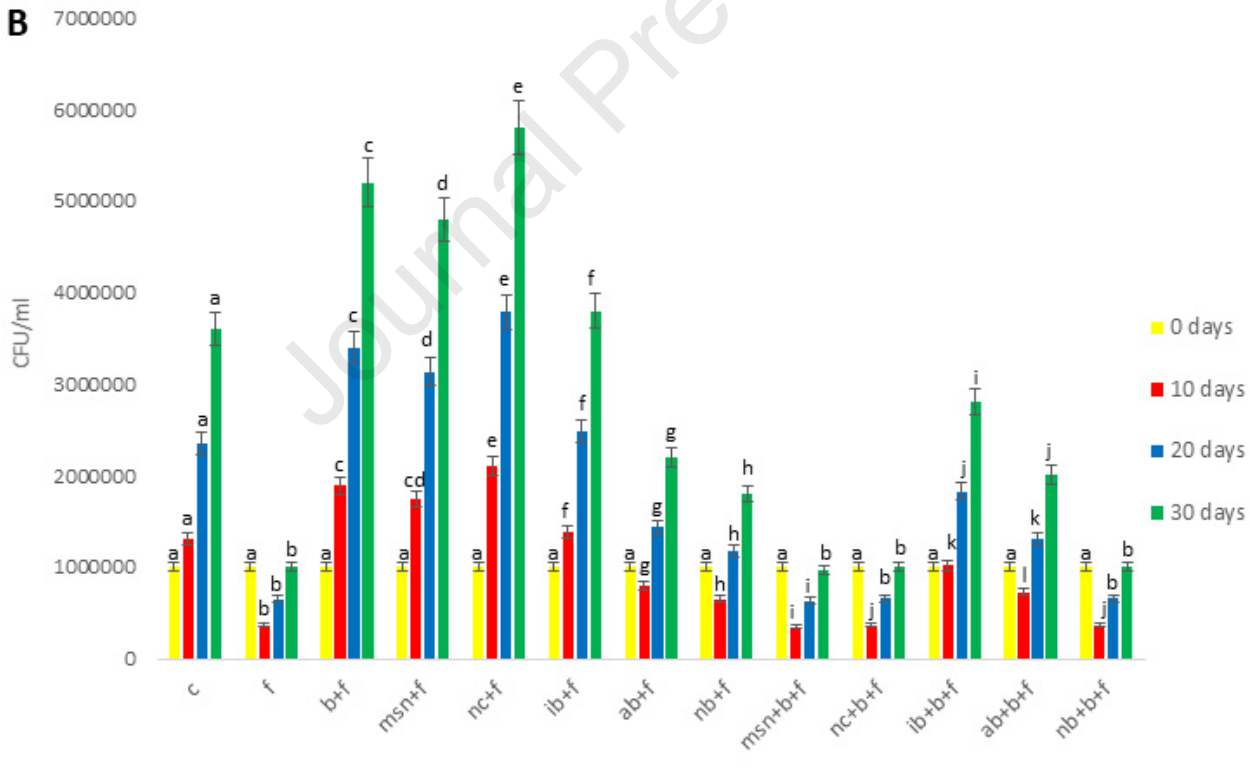












Highlights

- Fusarium infection causes loss of billions of dollars annually
- Plant growth promoting bacteria enhance properties of nanoparticles and biochar
- Application of these systems augments chlorophyll, nitrogen and phosphorus content
- Under such treatments antioxidative properties and viability of infected plants increase
- Field test will confirm efficacy of these systems as pesticides

Dac	laration	of interests	
Deci	iaralion	Of Interests	

☑ The authors declare that they have no known competing financial interests or personal relationships that could have appeared to influence the work reported in this paper.
\Box The authors declare the following financial interests/personal relationships which may be considered as potential competing interests:

John President